

RIGAKU VariMax Dual

Part 1 Measurement Manual with CrysAlis^{Pro}

X-ray Laboratory, Nano-Engineering Research Center, Institute of Engineering Innovation, The University of Tokyo

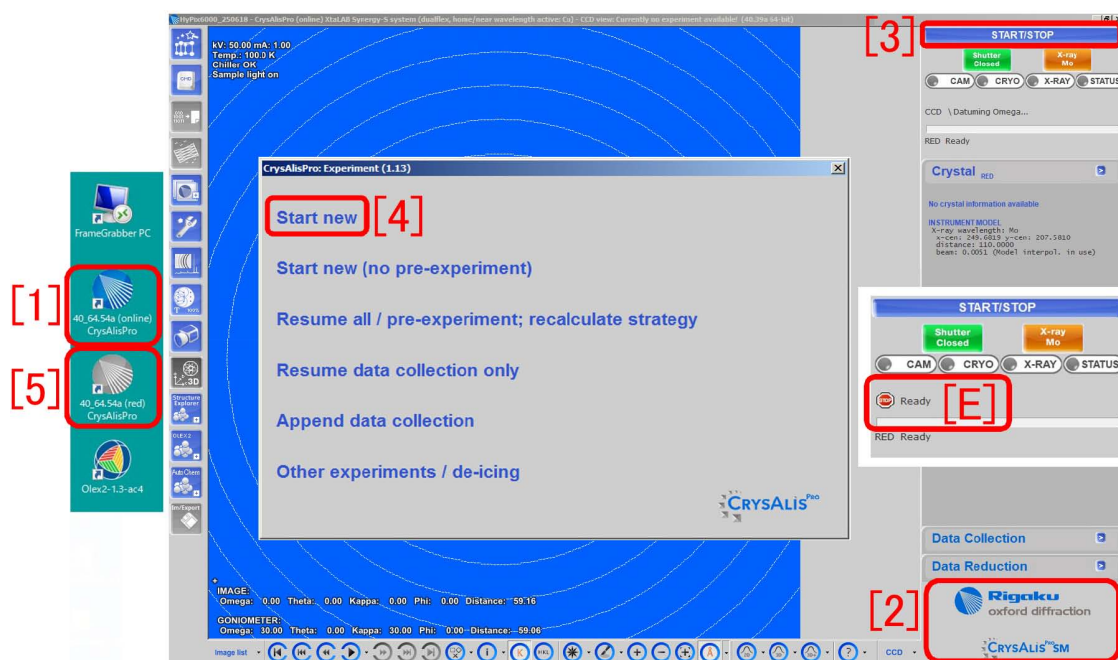


Figure 0: CrysAlis^{Pro} window collecting diffraction spots

This manual describes the usage of CrysAlis^{Pro} with which Rigaku VariMax Dual is controlled to obtain X-ray diffraction spots from small molecular-weight crystals. At first, '[1] 40.64.54a (online) CrysAlis^{Pro}' on the desktop of the computer should be double-clicked to start up CrysAlis^{Pro}. '[2] Small molecule / Protein switching button' should be 'CrysAlis^{Pro} SM'. If it is 'CrysAlis^{Pro} PX', it should be clicked to change to be the small-molecule mode. The software can be started by clicking '[3] START/STOP'. '[4] Start new' should be clicked to start the experiment.

'[5] 40.64.54a (red) CrysAlis^{Pro}' icon on the desktop can be double-clicked to start the off-line mode CrysAlis^{Pro}.

Appendix A [p.22] describes the reasonability of defining the reciprocal lattice. This is strongly recommended to read. The understanding of the reciprocal lattice is necessary for crystallography.

In Appendix B [p.26], how to determine the space group from consideration on extinction rules.

In Appendix C [p.39], the reason for representing reflection vectors with four indices and extinction rules for trigonal and hexagonal crystal systems.

Mathematical proofs for extinction rules described in Appendices B [p.26] and C [p.39] are recommended to read for further understanding of extinction rules when the reader has time.

Appendix D [p.45] describes how to obtain 3D outline shape of the crystal for numerical absorption correction.

When an error message as '[E]' on the right of Fig. 0 is displayed, it should be recovered referring to Appendix E [p.51].

Contents

1	Verification of humidity in the detector	1
1.1	Start up of the remote desktop	1
1.2	Start up of the camserver	1
1.3	Verification of the humidity in the detector	2
1.4	Close of the remote desktop	2
2	Choice or creation of the account	3
2.1	Startup of the CrysAlis ^{Pro}	3
2.2	Display of Pre-experiment window	3
2.3	Choice of the account	4
2.4	Creation of a new account	4
3	Mount and screening of the crystal	6
3.1	Mount of the crystal	6
3.2	Screening	8
4	WIT(What Is This)	10
4.1	Concerning ‘WIT’ (What Is This ?)	10
4.2	Performing ‘WIT’ (What is this ?)	11
4.3	Automatic setting of the strategy and starting the main measurement	11
5	Pre-Experiment	12
5.1	Start of Pre-Experiment	12
6	Main measurement and integration of the intensities after taking the outline of the crystal	14
6.1	Conformation of the strategy	14
6.2	Automatic taking crystal outline photos	17
6.3	The main measurement and integration of the diffraction intensities	17
6.4	Items to be set or confirmed during the main measurement	17
6.5	Finishing the experiment	19
A	Reasonability of defining the reciprocal lattice	22
A.1	Bragg’s reflection condition	22
A.2	Laue’s reflection condition	22
A.3	Ewald’s reflection condition (Ewald construction)	23
A.3.1	Foundation of Ewald construction	23
A.3.2	Relation between reciprocal lattice vector and Bragg reflection plane	24
A.4	Drawing of Miller and Miller indices	25

B	Determination of space group from extinction rule	26
B.1	Symmetric elements of crystal derived based on the group theory	28
B.2	Symbols of space groups	29
B.3	How to read extinction rules	30
B.4	Examples of extinction rules due to combinations of symmetric elements	31
B.4.1	Orthorhombic $P2_12_12_1$ (#19)	32
B.4.2	Monoclinic $P12_11$ [$P2_1$ (#4)]	32
B.5	Mathematical proofs of extinction rules	33
B.5.1	Extinction rules due to complex lattice	33
B.5.2	Extinction owing to glide axes	35
B.5.3	Extinction due to screw axes	36
C	Reflection indices and extinction rules in the cases of trigonal and hexagonal crystals	39
C.1	Cases of trigonal system	39
C.1.1	Diagram shown in <i>International Tables for Crystallography</i> (2006) Vol.A	39
C.1.2	Real and reciprocal coordinates	40
C.1.3	Derivation of extinction rule due to 3_1 screw axis	40
C.1.4	On the absence of extinction due to 2_1 screw axis perpendicular to c	41
C.2	Case of hexagonal system	42
C.2.1	Figure shown in <i>International Tables for Crystallography</i> (2006) Vol.A	42
C.2.2	Coordinates for describing six-fold screw axes	42
C.2.3	Derivation of extinction rule due to 6_1 screw axis	43
C.2.4	Derivation of the extinction due to 6_2 screw axis	44
C.2.5	Derivation of extinction rule due to 6_3 screw axis	44
D	Obtaining 3D data of the crystal shape	45
D.1	Abstract	45
D.2	Begining of making 3D data of crystal shape	45
D.3	Making a 'box' including the crystal	45
D.4	Trace of the crystal facet with T-shaped cursor	47
D.5	Cancellation of double registration of the crystal face	49
D.6	Edit of the crystal outline data	49
D.7	Registration of the crystal outline	50
E	Restart of the goniometer driver	51
E.1	Concerning the error of the goniometer driver	51
E.2	Shutdown and restart of the goniometer driver	51
E.3	Restart of the 'CrysAlis ^{Pro} '	51

List of Figures

0	CrysAlis ^{Pro} window collecting diffraction spots	i
1.1	Start up of the remote desktop	1
1.2	Start up of the software to control the FrameGrabber	1
1.3	Display of camserver(#1)	1
1.4	Display of the camserver(#2)	2
1.5	Display of the camserver(#3)	2
1.6	Close of the remote desktop	2
2.1	Initializing	3
2.2	Choice of the X-ray source	3
2.3	SM Screening window	3
2.4	Pre-experiment window	4
2.5	Folder selection window	4
2.6	Mount window	5
2.7	Change of the value of Theta	5
3.1	Magnet base and micromount	6
3.2	SM Screening window	6
3.3	Crystal mount window	6
3.4	Mount of the crystal	6
3.5	Around the goniometer head	7
3.6	Around the goniometer head	7
3.7	SM Screening window	7
3.8	Screening option window	8
3.9	Result of screening	8
3.10	Level of screening result	8
4.1	SM Screening window	10
4.2	WIT window	10
4.3	Molecular model	10
4.4	Molecular model	11
4.5	Measurement menu	11
5.1	SM Screening window	12
5.2	SM Screening window	12
5.3	Diffraction spots	12
6.1	Strategy window	15
6.2	Hand switch of the illumination	15
6.3	Options of the strategy	15
6.4	Strategy window	16

6.5	Optical image window of the crystal	16
6.6	Menu of Crystal tab has been opened by clicking '>'	16
6.7	Typing of the molecular formula	17
6.8	Typing of the comment	17
6.9	Input of the crystal information	17
6.10	Crystal live view	18
6.11	The main measurement schedule and status in progress	18
6.12	Menu shown after finishing the data collection	18
6.13	Message displayed during waiting the CCD stops	18
6.14	Menu of finalize	18
6.15	Finalize option	19
6.16	A message 'There is no photo of the crystal'	19
6.17	Selection of the space group	19
6.18	Shutdown options	20
6.19	X-ray power is ramping down	20
A.1	Bragg's reflection condition.	22
A.2	Laue's reflection condition.	23
A.3	Ewald sphere	24
A.4	Drawing of Miller and Miller indices	25
B.1	Content of 'process.out' (#1). [Taurine; monoclinic $P2_1/c$ (#14)].	26
B.2	Content of 'process.out' (#2). [Taurine; monoclinic $P2_1/c$ (#14)]	26
B.3	Content of 'process.out' (#3) [Taurine; monoclinic $P2_1/c$ (#14)]. [setting #1] corresponds to '[1] CELL CHOICE 1' in Fig. B.5.	27
B.4	Reflection condition of $P2_1/c$ (#14) described in <i>International Tables for Crystallography</i> (2006) Vol.A. $0k0$ reflections when k is odd and, $h0l$ and $00l$ reflections when l is odd, extinguish.	27
B.5	Drawings for space group $P2_1/c$ (#14) in <i>International Tables for Crystallography</i> (2006) Vol.A. Protein crystals do not belong to this space group absolutely.	29
B.6	Redesignation of space group in CrystalStructure 4.1. (in the case of small molecular-weight crystal).	31
B.7	Drawing for $P\bar{1}$ (#2) in <i>International Tables for Crystallography</i> (2006) Vol.A. Since this space group has symmetric center, protein crystals do not belong to it. The phase problem is simple (0 or π (180°)).	31
B.8	Drawing for $C12/c1[C2/c]$ (#15) in <i>International Tables for Crystallography</i> (2006) Vol.A. Protein crystals do not belong to this space group absolutely since it has glide plane.	31
B.9	<i>International Tables for Crystallography</i> (2006) Vol.A $P2_12_12_1$ (#19).	32
B.10	<i>International Tables for Crystallography</i> (2006) Vol.A $P12_11[P2_1]$ (#4).	32
C.1	<i>International Tables for Crystallography</i> (2006) Vol.A, Symmetric elements. $P3_121$ (#152).	39
C.2	<i>International Tables for Crystallography</i> (2006) Vol.A, Positions of atoms. $P3_121$ (#152).	39
C.3	Real (black) and reciprocal (gray) primitive translation vectors.	40
C.4	<i>International Tables for Crystallography</i> (2006) Vol.A, Symmetric elements. $P6_122$ (#178).	42
C.5	<i>International Tables for Crystallography</i> (2006) Vol.A, Positions of atoms. $P6_122$ (#178).	42
D.1	Menu of 'Crystal tab'	45

D.2	Initial window of making the crystal outline data	46
D.3	Optical image window of the crystal (#1)	46
D.4	Tool window #1	46
D.5	Optical image window of the crystal (#2)	47
D.6	Optical image window of the crystal (#3)	47
D.7	Tool window #2	47
D.8	Optical image window of the crystal (#4)	47
D.9	'T-shaped cursor' in Fig. D.8 has been right-clicked	48
D.10	Add face window (#1)	48
D.11	Tool window #3	48
D.12	Optical image window of the crystal (#5)	48
D.13	Add face window (#2)	48
D.14	Tool window #4	48
D.15	Optical image window of the crystal (#6)	49
D.16	Add face window (#3)	49
D.17	Tool window #5	49
D.18	Tool window #6	49
D.19	Tool window #7	50
D.20	Optical image window of the crystal (#7)	50
E.1	Error message of the goniometer driver	51
E.2	The whole figure of the apparatus	51
E.3	The goniometer driver	51

Chapter 1

Verification of humidity in the detector

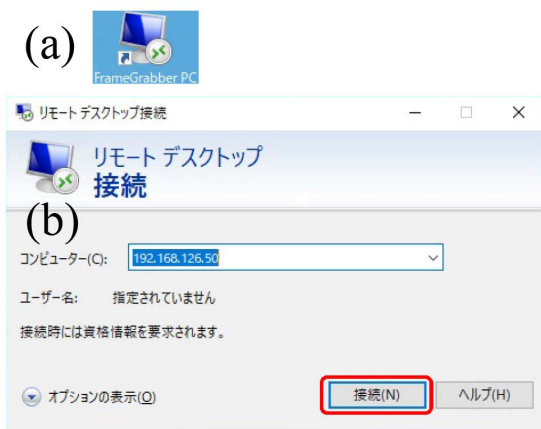


Figure 1.1: Start up of the remote desktop

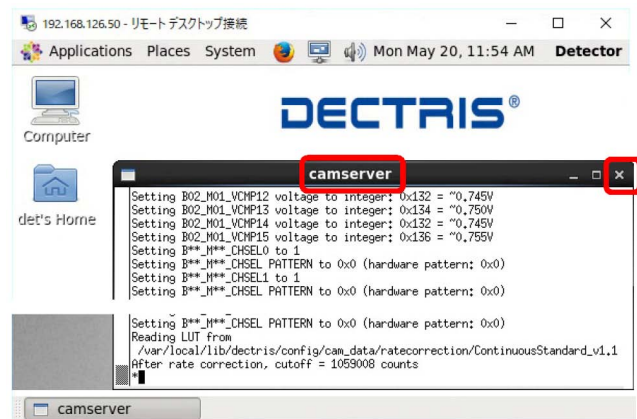


Figure 1.3: Display of camserver(#1)

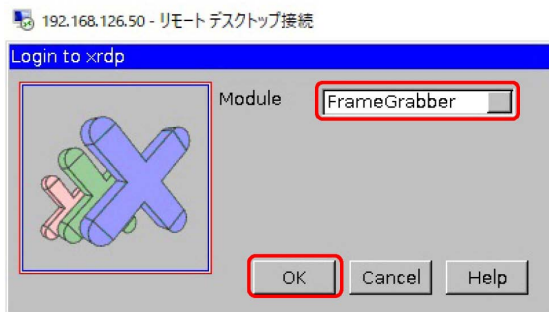


Figure 1.2: Start up of the software to control the FrameGrabber

Inside the high-speed two-dimensional detector PILATUS, dry nitrogen circulates such that the humidity in it is less than 25%. It is necessary to verify that the value of humidity in the detector is sufficiently low.

1.1 Start up of the remote desktop

The icon of 'FrameGrabber PC' in Fig. 1.1 (a) should be clicked to let Fig. 1.1 (b) be displayed.

'FrameGrabber PC' is a server computer to control the detector. Its IP is 192.168.126.50. After verifying this IP, 'Connect (N)' should be clicked to start up the remote desktop as shown in Fig. 1.2.

1.2 Start up of the camserver

In Fig. 1.2, 'OK' should be clicked with 'FrameGrabber' selected in the pull-down menu to let the window of 'camserver' (a software to control the PILATUS) be displayed as shown in Fig. 1.3.

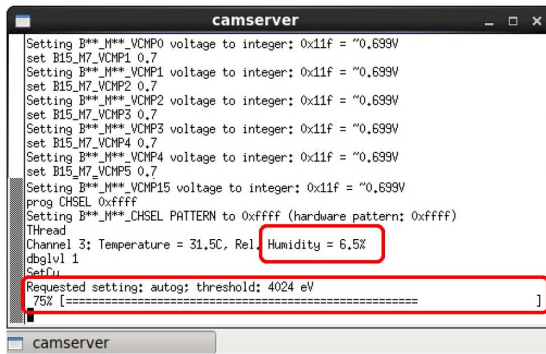


Figure 1.4: Display of the camserver(#2)

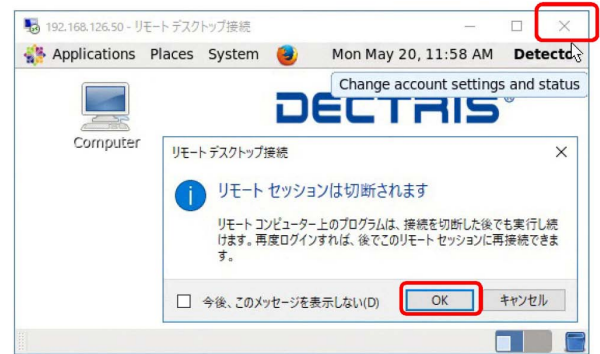


Figure 1.6: Close of the remote desktop

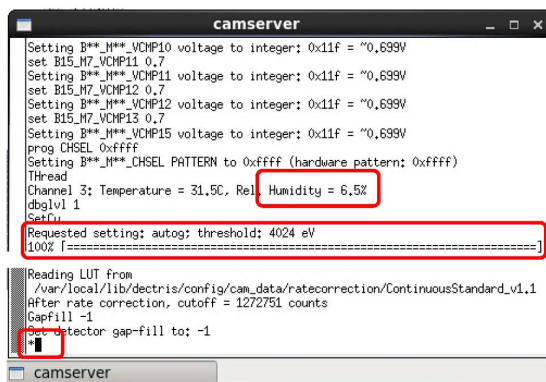


Figure 1.5: Display of the camserver(#3)

1.3 Verification of the humidity in the detector

In Fig. 1.3 [p. 1], '×' on the upper right corner

of 'camserver' should be clicked to close this window. Then, this window is automatically displayed again as shown in Fig. 1.4. Here, the value of the humidity has been displayed to be 6.5 % and a bar graph under 'Requested setting' stretches to the right direction. When it reaches to 100 %, Fig. 1.5 is displayed showing the value of humidity again (6.5 %) at the center. If it is over 25 %, call the manager, please (K. Okitsu, 27470, 090-2203-8789) since the detector does not work with such a high value of humidity

1.4 Close of the remote desktop

After confirming the value of humidity in Fig. 1.5, the remote desktop should be closed by clicking '×' on the upper right corner of Fig. 1.6 and then 'OK' in the message window.

Chapter 2

Choice or creation of the account



Figure 2.1: Initializing

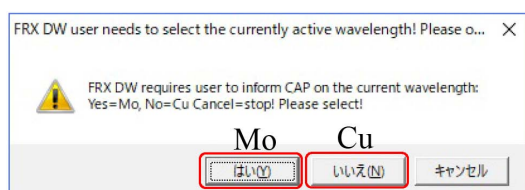


Figure 2.2: Choice of the X-ray source

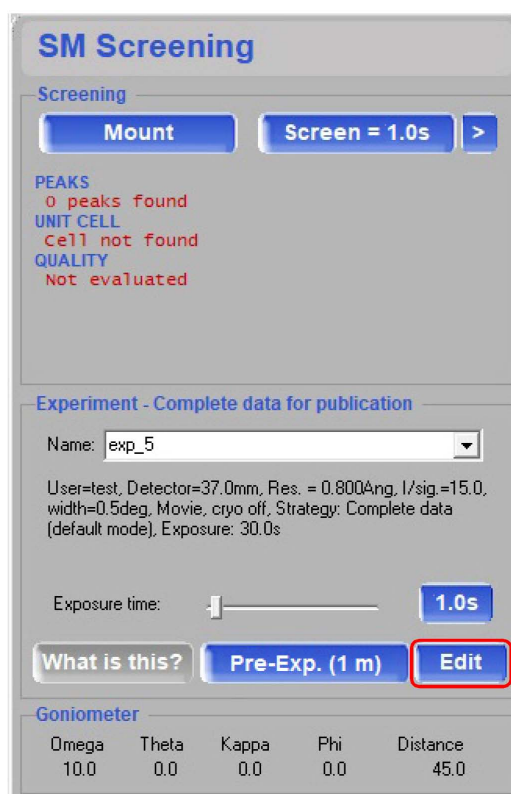


Figure 2.3: SM Screening window

2.1 Startup of the CrysAlis^{Pro}

If an icon of CrysAlis^{Pro} as shown in Fig. 0 (a) '[1]' or '[5]' exits on the task bar of the Windows, it should be closed.

By double-clicking '[1] 40.64.50a (online) CrysAlis^{Pro}', CrysAlis^{Pro} can be started. '[2] Protein / Small molecule switching button' should be 'CrysAlis^{Pro} SM'. If it is 'CrysAlis^{Pro} PX', it should be clicked to change to 'CrysAlis^{Pro} SM'.

At first, the apparatus is initialized for several minutes. During that, Fig. 2.1 is displayed. 'CCD / Datuming Chi ...' in the red frame means that the angle of χ is being obtained.

After waiting several minutes, a message 'CCD Ready' and Fig. 2.2 appear. 'Yes' for Mo and 'No' for Cu X-ray source should be clicked.

'[3] START/STOP' on the upper right corner of Fig. 0 on the cover, should be clicked to start the software to display 'SM Screening tab' as shown in Fig. 2.3.

2.2 Display of Pre-experiment window

Click 'Edit' on the lower right of 'SM Screen tab', please, to display 'Pre-experiment window'

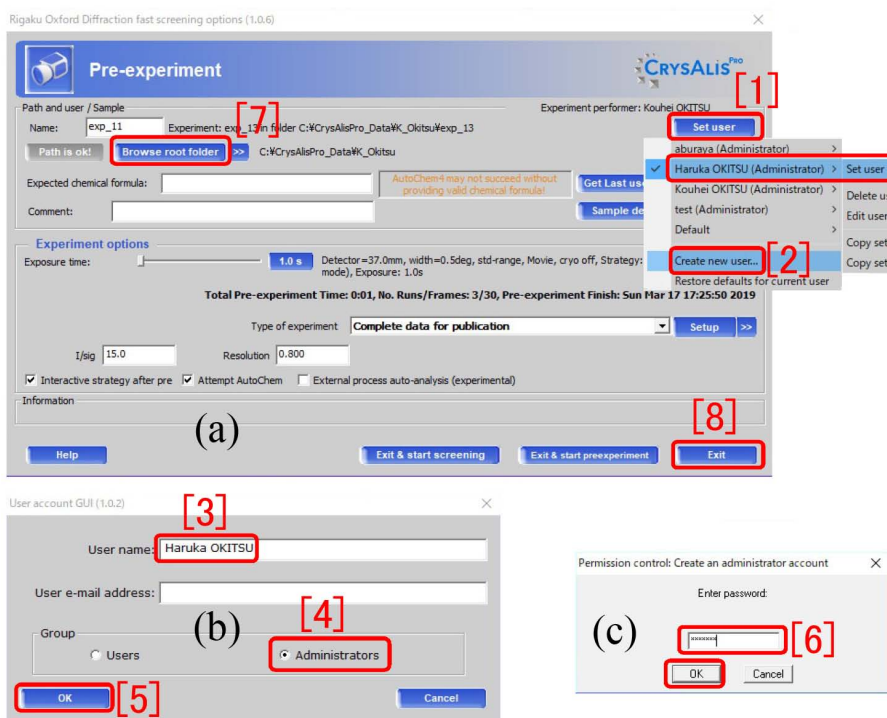


Figure 2.4: Pre-experiment window

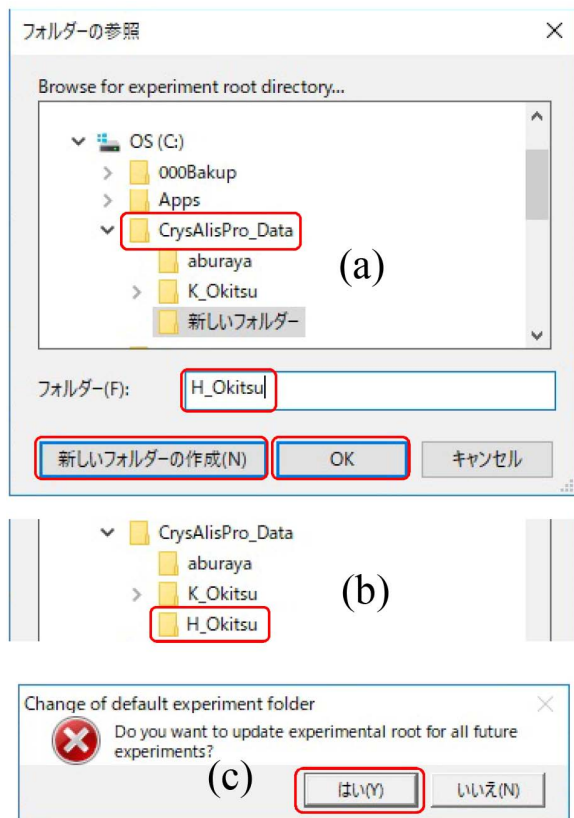


Figure 2.5: Folder selection window

as shown in Fig. 2.4

2.3 Choice of the account

If the user account has been created, '[1] Set user' on the upper right corner of Fig. 2.4 should be clicked to open the pull-down menu from which the account can be selected. When the password is asked as shown in Fig. 2.4 (c), 'ccdbest' should be typed. Then, '[8] Exit' can be clicked for closing the 'Pre-experiment window' to go to the next chapter 'Mount and screening of the crystal'.

2.4 Creation of a new account

Fig. 2.4 '[1]-[7]' should be clicked in this order to create a new account.

At first, '[1] Set user' on the upper right of Fig. 2.4 should be clicked to open the pull-down menu from which '[2] Create new user' can be clicked to select. Then in Fig. 2.4 (b), the user name should be typed in '[3]', '[4] Administrator' should be checked to click '[5] OK'. When the password is asked as shown in Fig. 2.4 (c), 'ccdbest' should be typed to click 'OK'.

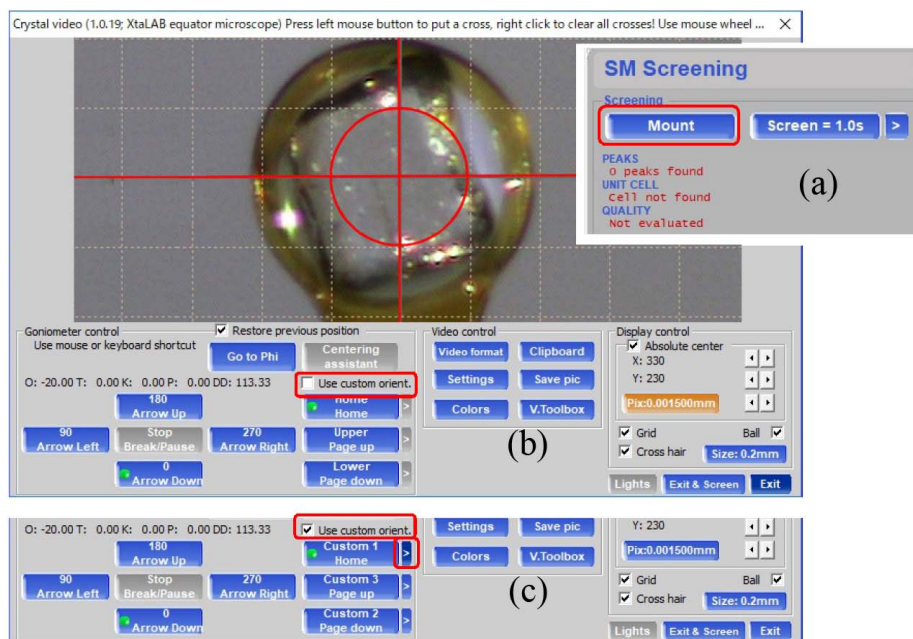


Figure 2.6: Mount window

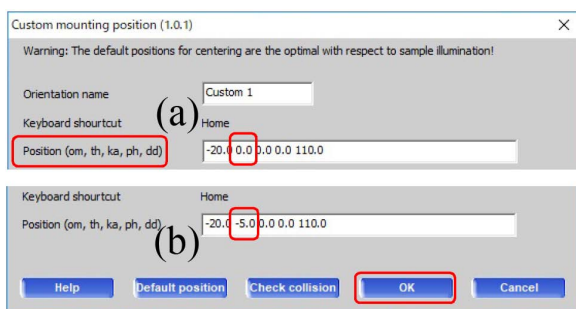


Figure 2.7: Change of the value of Theta

[7] Browse root folder' at the center of Fig. 2.4 (a) can be clicked to open the file explorer as shown in Fig. 2.5 (a). After choosing a root folder in which to create a new folder in Fig.

2.5 (a), 'Create new folder (N)' can be clicked to type the new folder name. After typing it and clicking 'OK', Fig. 2.5 (b) is displayed. In Fig. 2.5 (c), 'Yes (Y)' can be clicked to let it be the root folder. Then, '[8] Exit' in Fig. 2.4 (a) should be clicked to close the 'Pre-experiment window'.

'Mount' of 'SM Screening tab' in Fig. 2.6 (a) can be clicked to open the crystal mount window as shown in Fig. 2.6 (b). After checking 'Use custom orient.' as shown in Fig. 2.6 (c), '>' on the right of 'Custom1' should be clicked to open Fig. 2.7. Here, the second parameter should be changed to be -5.0 as shown in Fig. 2.7 (b) and 'OK' can be clicked to finish creating a new account to go to the next chapter 'Mount and screening of the crystal'.

Chapter 3

Mount and screening of the crystal

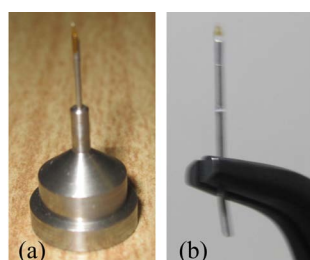


Figure 3.1: Magnet base and micromount

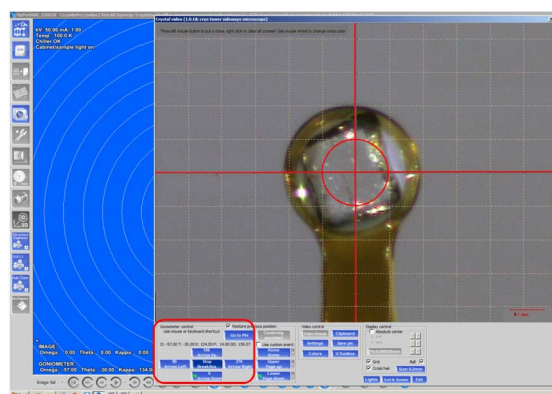


Figure 3.3: Crystal mount window

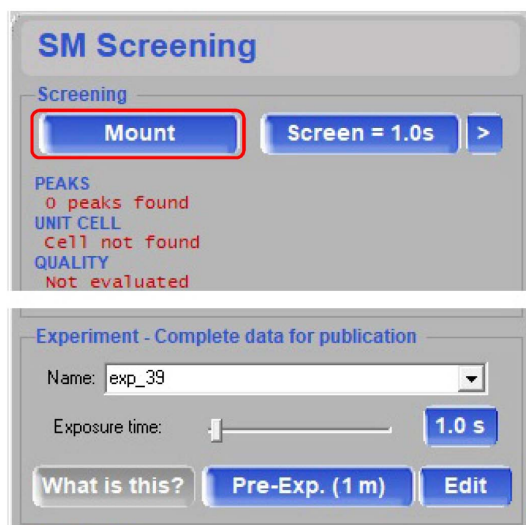


Figure 3.2: SM Screening window



Figure 3.4: Mount of the crystal

3.1 Mount of the crystal

Fig. 3.1 (a) shows a magnet mount base whose diameter is ~ 10 mm. There are two types of mount bases. If a straight stem of micromount cannot be fixed just inserting it to the mount

base, it should be slightly bent by using a radio plier such that it can be elastically fixed.

Fig. 3.2 show the 'SM Screen window' on the right of the window. 'Mount' on the upper left of Fig. 3.2 can be clicked to open Fig. 3.3.

In Fig. 3.4, the nozzle of cooled N_2 blower is covered with a card. The crystal is recommended to cool rapidly by removing the card

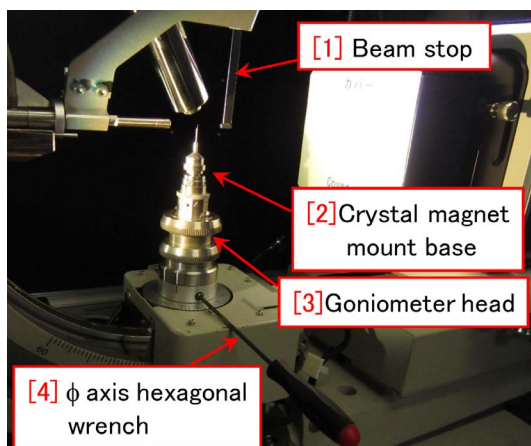


Figure 3.5: Around the goniometer head

after mounting it. However, the center of the ring of micromount can be adjusted to be at the cross line before mounting the crystal to the micromount to cool the crystal rapidly later.

Fig. 3.5 shows around the goniometer head on which the crystal is mount. The ϕ axis can be rotated manually by unfastening '[4] ϕ axis hexagonal wrench'. After unfastening Fig. 3.6 '[1] Height adjuster clump', '[3] Height adjuster ring' can be rotated with '[2] Driver' to adjust the height of the crystal. When adjusting the crystal position, '[4] Detector cover' should be put in front of the detector. **the receiving surface of the detector should not be touched.** After adjusting the height of the crystal, '[1] Height adjuster clump' should be fastened. However, it should not be fastened too strongly such that the small hexagonal screw is not broken. Horizontal X Y position should be adjusted with the box wrench on the opposite side of the '[2] Driver' by rotating X Y adjuster screws.

After adjusting the X, Y and Z positions of the micromount, the crystal should be mounted to the micromount by viewing it under the microscope. With regard to the usage of the microscope, refer to Appendix B of Part 0 manual, please. With regard to how to mount the crystal to the micromount, it should be done according to the style depending on the user's group.

In the case where the crystals are in a solution, they can be sucked up in a Pasteur pipette and dropped on a slide glass on which they can be moved to another drop of liquid paraffin.

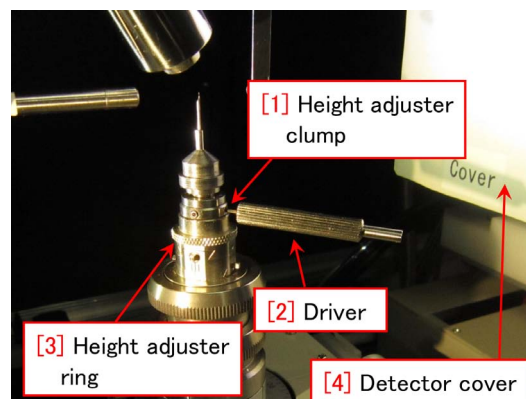


Figure 3.6: Around the goniometer head

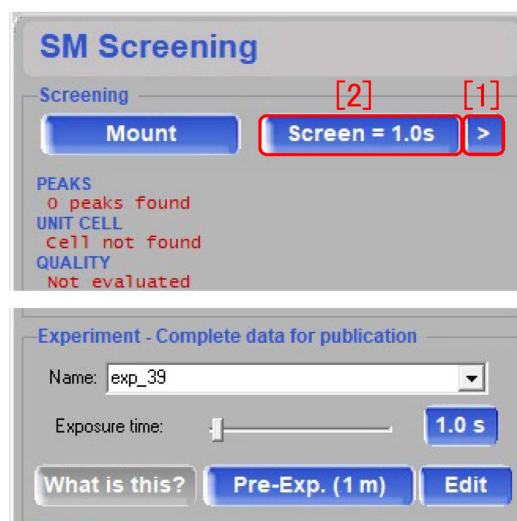


Figure 3.7: SM Screening window

A crystal with a proper size can be skimmed to the micromount from there in general. The crystal should be mounted with the liquid paraffin whose amount should be decreased to be as small as possible. Liquid paraffin is frozen without being crystallized by blown in the cooled N_2 .

After putting the crystal to the micromount, the magnet mount should be magnetically put on the goniometer head. The crystal should be around the cross line since the micromount has been approximately adjusted to the correct position. The crystal position should be strictly adjusted in the same way as previously described as rapidly as possible. The surface of the micromount is recommended to be parallel

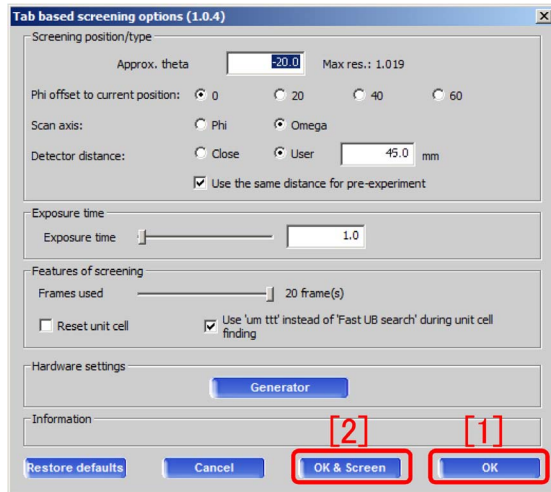


Figure 3.8: Screening option window

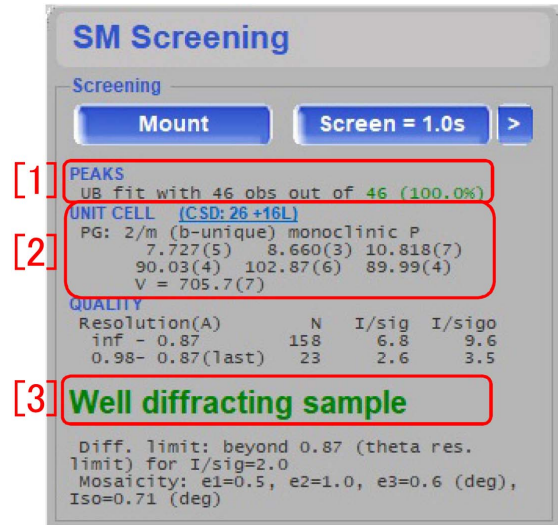


Figure 3.9: Result of screening

to the direction of X or Y such that the position can easily be adjusted.

3.2 Screening

Fig. 3.6 [p. 7] '[4] Detector cover' should be removed carefully **such as no to touch the detector surface**.

The screening process is done to estimate the crystal quality. Here, it should be verified that diffraction spots with sufficient intensities can be obtained.

Fig. 3.7 [p.7] shows a 'SM Screening window' displayed on the right of the screen. By clicking '[1]>' on the upper right, 'Screening option window' of Fig. 3.8 can be displayed. With the items set as shown as this. By clicking '[2]OK & Screen' in Fig. 3.8 or clicking '[1]OK' and then '[2]Screen = 1.0s' in Fig. 3.7 [p. 7], screening can be started.

After finishing the screening, Fig. 3.9 is shown. It is shown that 46 diffraction

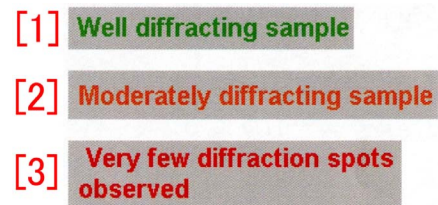


Figure 3.10: Level of screening result

spots were observed all of them have been successfully assigned to reflection indices at '[1]', that the crystal system may be monoclinic at '[2]' and that sufficiently strong intensities were obtained at '[3]'. In this case, go to the next chapter 'WIT', please.

When Fig. 3.10 '[2]' or '[3]' is shown and '[1]Well diffraction sample' is not shown, another crystal should be retried since the quality of the crystal is not sufficient.

To be continued

Chapter 4

WIT(What Is This)

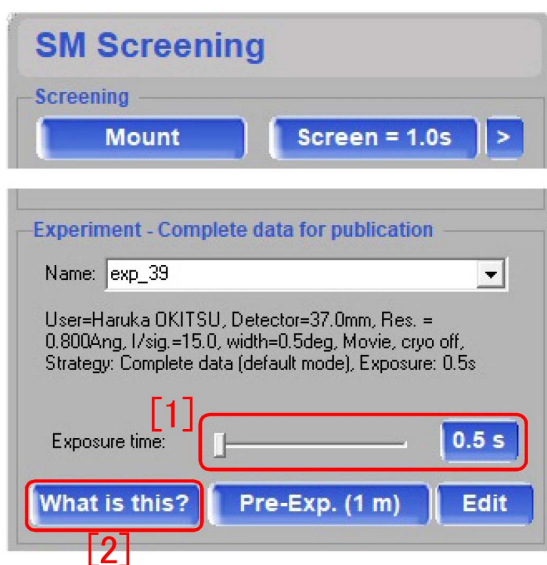


Figure 4.1: SM Screening window

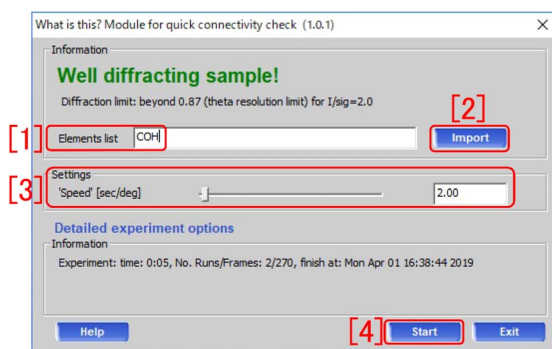


Figure 4.2: WIT window

4.1 Concerning 'WIT' (What Is This ?)

The purpose of 'WIT' is to determine the molecular structure rapidly by using the function of 'AutoChem'.

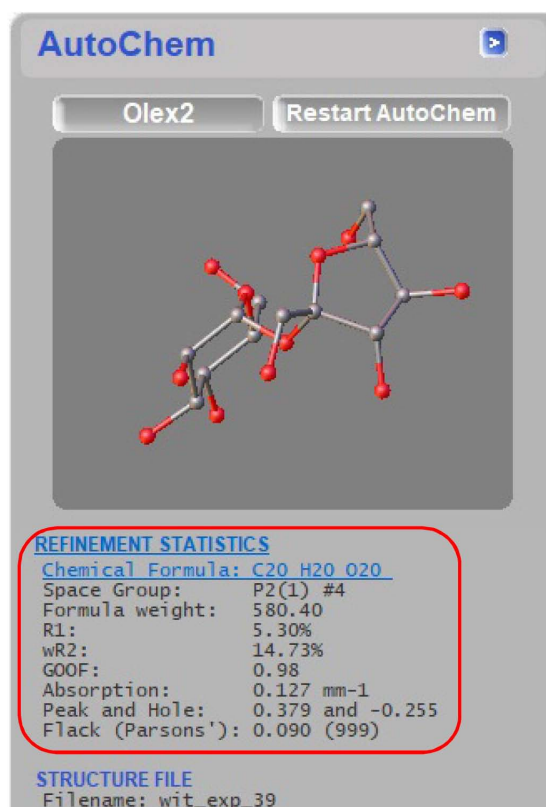


Figure 4.3: Molecular model

In the case of Mo X-ray source, The main measurement can be set just after finishing 'WIT' since the exposure time has been estimated for sufficient resolution range as high as 0.8 Å.

However, in the case of Cu X-ray source, the highest resolution of 'WIT' is around 1.0 Å and is not sufficient. Then after finishing 'WIT', 'Pre-experiment' should necessarily be done to estimate the exposure time also for sufficiently high resolution range (0.8 Å). Therefore, the exposure time should be estimated by doing the Pre-

experiment even when the molecular structure has been determined by the 'WIT'.

The WIT is not recommended to collect the diffraction data for publication since it has been scheduled rapidly to obtain the molecular structure with low precision.

4.2 Performing 'WIT' (What is this ?)

Fig. 4.1 on the right of the screen is 'SM Screening window'. The proper exposure time does not have to be set in '[1]' of Fig. 4.1 since it has been estimated in the screening.

'AutoChem' on the OLEX² attempts to determine the molecular structure under the assumption that the molecule has atoms of C, H, N and O. Then, the molecular structure having only these elements is sometimes determined even if the textbox of Fig. 4.2 '[1]' is empty. However, atomic symbols of elements that the molecule has, should be typed in general particularly when it has elements other than C, H, N and O. When they are the same as the previous experiment, '[2] Inport' can be clicked to set them.

As shown in Fig. 4.3 and Fig. 4.4, molecular model is shown and is improved to the correct structure.

The correct molecular formula is 'C₁₂H₂₂O₁₁' (sucrose), the correct crystal system and space group are monoclinic and *P*2₁. With regard to the space group, Appendix B [p.26] can be referred to. There are two molecules in the unit cell.

In Fig. 4.3, the molecular formula is wrong and the space group is right. In Fig. 4.4, Numbers of carbon (C) and oxygen (O) are right, number of hydrogen (H) is wrong and the space group is right.

4.3 Automatic setting of the strategy and starting the main measurement

After the WIT finishes, '[3] START/STOP' in Fig. 0 on the cover of this manual should be clicked to show Fig. 4.5. Here, 'Start new (based on solved structure)' can be clicked to start the

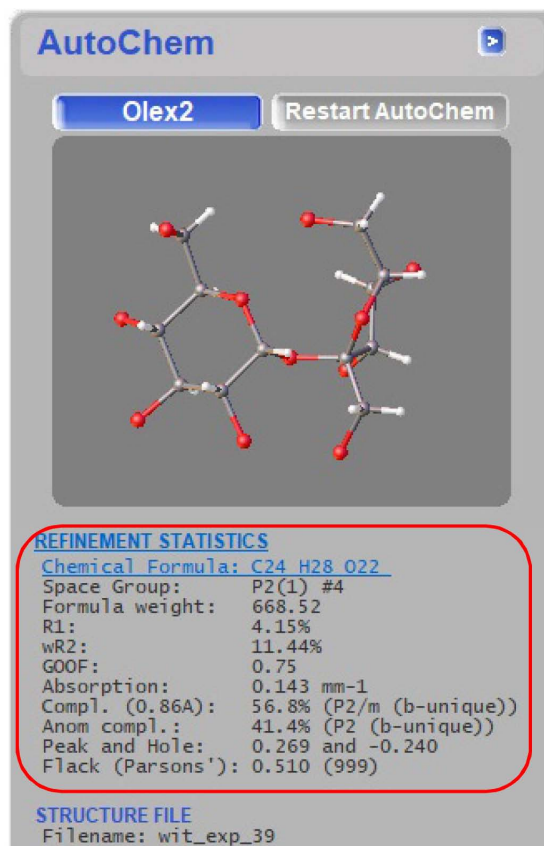


Figure 4.4: Molecular model

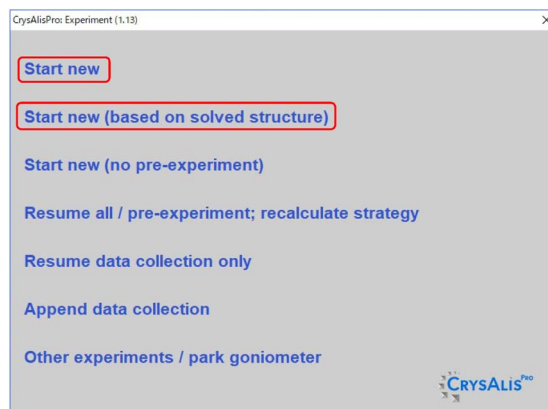


Figure 4.5: Measurement menu

main measurement when the X-ray source is Mo as described in chapter 6 [p.14]. However, when the X-ray source is Cu, Pre-experiment should be done after clicking 'Start new' on the uppermost part of Fig. 4.5 as described in the next chapter 4 since the proper exposure time has not been estimated for sufficient resolution range (0.8 Å).

Chapter 5

Pre-Experiment

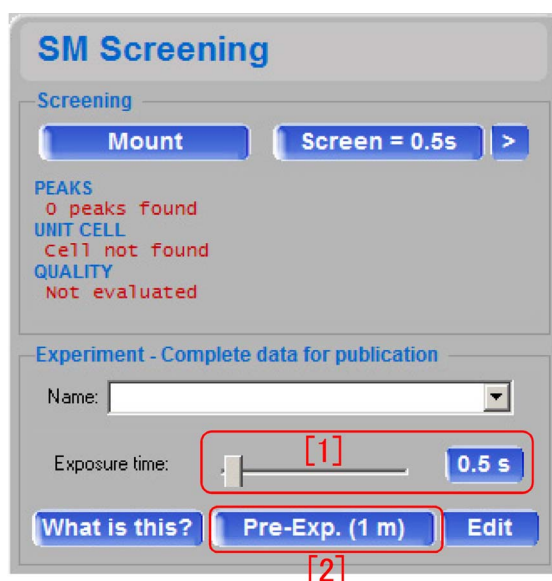


Figure 5.1: SM Screening window

5.1 Start of Pre-Experiment

When the X-ray source is Mo, Pre-Experiment does not have to be done. However, it is Cu, Pre-Experiment should be done.

Fig. 5.1 is ‘SM Screening window’ shown on the right of the screen. By clicking ‘0.5s’ of [1] or sliding it, the exposure time can be set.

‘1m’ of [2]Pre-Exp.(1m) in Fig. 5.1 means that the Pre-Experiment takes 1 min. [2]Pre-Exp.(1m) can be clicked to start the Pre-Experiment. Status of the Pre-Experiment is

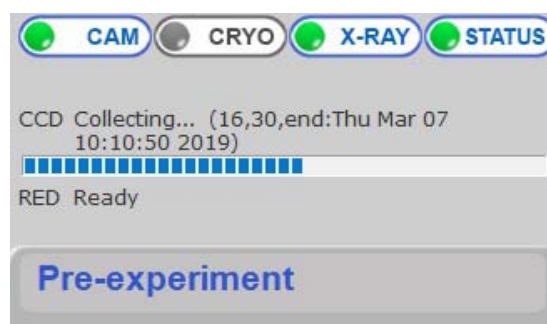


Figure 5.2: SM Screening window

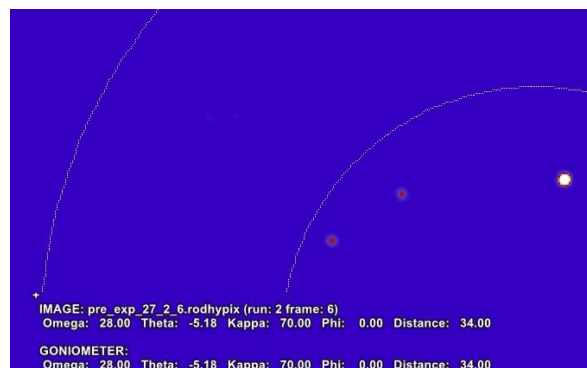


Figure 5.3: Diffraction spots

displayed as shown in Fig. 5.2

During the Pre-Experiment, the diffraction spots are displayed as shown in Fig. 5.3.

After the Pre-Experiment finishes, the strategy for the main experiment is automatically calculated as shown in Fig. 6.1 [p.15].

To be continued

Chapter 6

Main measurement and integration of the intensities after taking the outline of the crystal

6.1 Conformation of the strategy

Fig. 6.1 is ‘Strategy window’ displayed after the WIT and/or the Pre-experiment. In the red frame on the upper left corner, parameters to devise the strategy for the main measurement have been set.

To obtain optical images of the crystal, the hand switch in front of the computer display as shown in Fig. 6.1, should be turned on.

In the red frame of ‘[1]’ in Fig. 6.1, one of the radio button of ‘Resolution’, ‘Theta’ or ‘2Theta’ should be checked to set the resolution.

Under the frame of ‘[1]’, there are radio buttons ‘Laue group’ and ‘Other’. ‘Laue group’ has been checked and ‘2/m’ has been selected from the pull-down menu based on the result of WIT and/or Pre-Experiment. Laue group is the groups categorized based on the symmetry of reciprocal lattice. ‘2/m’ is a Laue group of the monoclinic space group (refer to the leftmost column in Table B.1 [p.27]). When the reciprocal lattice has high symmetry, since there are many equivalent indices of reflection, both ‘Completeness’ (how many reflections to obtain the resolution are measured) on the left ordinate and ‘Redundancy’ (how many equivalent reflections are measured redundantly) on the right ordinate in lower left red frame ‘[5]’ are high. ‘Coverage’ on the left ordinate and ‘Redundancy of coverage’ on the right ordinate in lower right red frame ‘[6]’ are completeness

and redundancy, respectively when there are no equivalent reflection indices owing to the assumption of the space group of $P1$ with the lowest symmetry. Fig. 6.1 Check box ‘Friedel mates are equivalent . . .’ should be checked when averaging the Friedel mates. Friedel mates are pairs of $h k l$ and $\bar{h} \bar{k} \bar{l}$ reflections. Absolute values of structure factors $F_{h k l}$ and $F_{\bar{h} \bar{k} \bar{l}}$ are identical since they are complex conjugate according to Friedel’s law. However, $F_{h k l}$ and $F_{\bar{h} \bar{k} \bar{l}}$ are dealt with not to be complex conjugate and then do not give the same reflection intensities when considering absorption of X-rays in the crystal except when the crystal has the symmetric center. By taking advantage of this, the absolute structure of chiral molecule, i.e. which the molecule is L- or D-body (S- or R-body), can be determined. In such a case, Fig. 6.1 [1] ‘Friedel mates are equivalent . . .’ should be unchecked.

‘Detector Distance’ is the distance between the crystal and the detector surface should be greater than 35 mm. It’s recommended value is 45 mm.

‘[2] Scan width’ in Fig. 6.1 is so-called oscillation angle [deg]. While the renewed system of VariMax Dual takes X-ray intensities of diffraction spots continuously measured without closing the shutter, an X-ray diffraction image taken on the detector ‘PILATUS’ during rotating the goniometer by the oscillation angle, is dealt with as one shot. In the old system of VariMax Dual, the shutter was opened

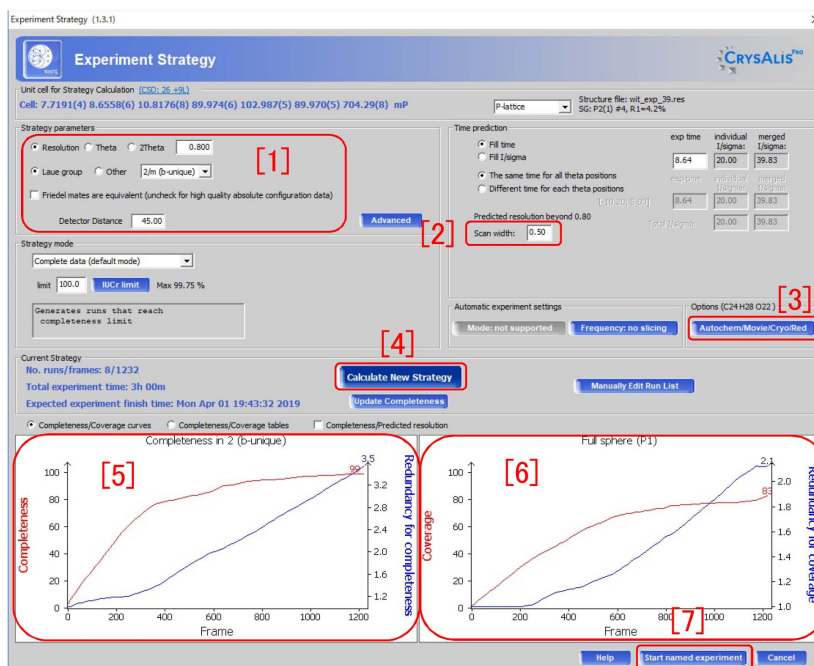


Figure 6.1: Strategy window



Figure 6.2: Hand switch of the illumination

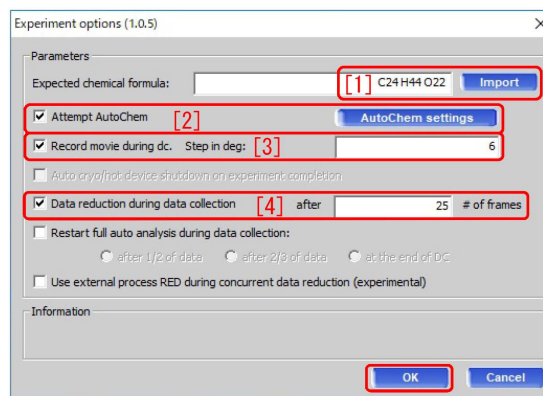


Figure 6.3: Options of the strategy

during the goniometer rotates by '[2] Scan width'. The value in Å or in deg should be set in the text box. Theta (θ) is the Bragg angle and 2Theta is $2 \times \theta$. In further older systems of single crystal diffractometer, the goniometer angle was oscillated during the shutter opens. '[2] Scan width' was called 'oscillation angle'.

By clicking '[3] AutoChem/Movie/Cryo/Red' in Fig. 6.1, Fig. 6.3 is displayed. Here, the molecular formula in '[1]' should be input, 'Attempt AutoChem [2]' should be checked, 'Record movie during dc [3]' should be

checked, and angular step when taking photos of the crystal with an integer (1 ~ 6) [deg] should be typed. If the parameters in Fig. 6.1 were changed, '[4] Calculate New Strategy' at the center of Fig. 6.1 should be clicked after that. '[7] Start named experiment' on the lower right of Fig. 6.1 can be clicked to open Fig. 6.4 [p.16]. In Fig. 6.4, [p.16] the molecular formula should be typed in the text box of '[1] Expected chemical formula' if it is known. '[2] Start' can be clicked to start the main measurement after automatically taking

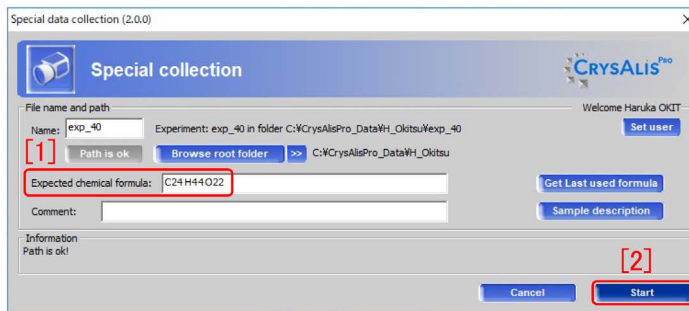


Figure 6.4: Strategy window

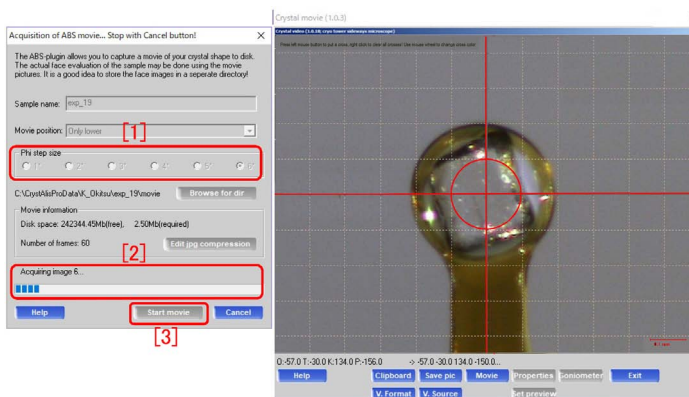


Figure 6.5: Optical image window of the crystal

optical photo of outline data of the crystal.

With regard to how to make 3D outline shape data, the descriptions in Appendix D [p.45] should be referred to.

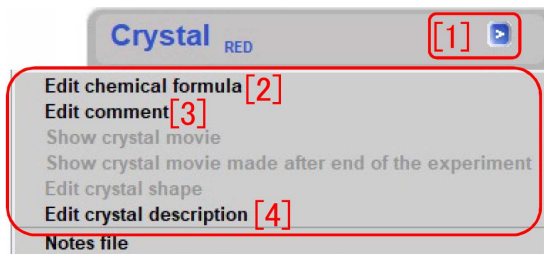


Figure 6.6: Menu of Crystal tab has been opened by clicking '>'

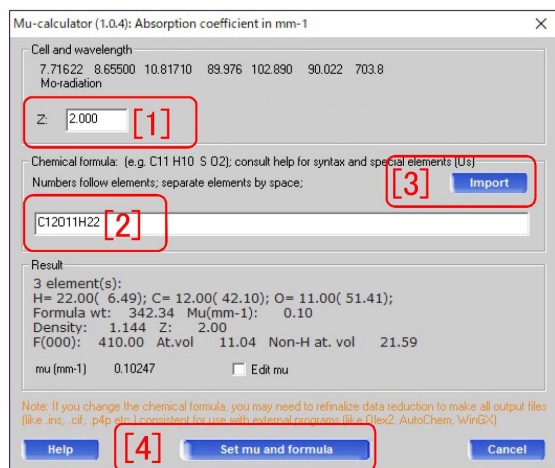


Figure 6.7: Typing of the molecular formula



Figure 6.8: Typing of the comment

6.2 Automatic taking crystal outline photos

Before starting the main measurement, ‘Optical window of the crystal outline’ of Fig. 6.5 opens to take outline photos of the crystal. Fig. 6.5 ‘[2]’ shows the status of progress as a bar chart.

When the outline photos are taken manually, after setting the step with which the goniometer is rotated, by checking one of the radio buttons of ‘[1] 1 ~ 6’. ‘[3] Start movie’ can be clicked to start taking outline photos of the crystal.

6.3 The main measurement and integration of the diffraction intensities

After taking outline photos of the crystal, the main measurement automatically stars.

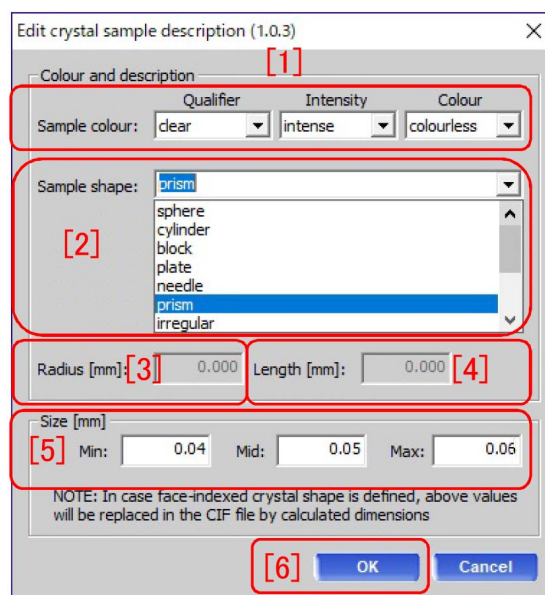


Figure 6.9: Input of the crystal information

6.4 Items to be set or confirmed during the main measurement

In Fig. 6.6, ‘[1] >’ on the right of ‘Crystal tab’ can be clicked to open a menu window in which ‘[2]’, ‘[3]’ and ‘[4]’ are included. These can be clicked to open Figs. 6.7, 6.8 and 6.9.

In Fig. 6.7 that has been opened by clicking ‘Edit chemical formula [2]’ in Fig. 6.6, the number of molecule whose molecular formula as shown in ‘[2]’, is ‘Z [1]’ in one unit cell. ‘[3] Import’ can be clicked to load the same values as the previous experiment. ‘[4] Set mu and formula’ should be clicked to set the input values.

In Fig. 6.8 that has been opened by clicking Fig. 6.6 ‘Edit comment [3]’, the comment can be typed to be set by clicking ‘OK’.

When the crystal shape is approximated with a rectangular solid, the sizes can be set in ‘[5]’ of Fig. 6.9 that has been opened by clicking ‘Edit crystal description [4]’ in Fig. 6.6. ‘Qualifier’, ‘Intensity’ and ‘Colour’ can be selected from the pull-down menu of Fig. 6.9 ‘[1]’. From ‘[2]’, shape of the crystal can be selected. If ‘Sphere’ is selected, ‘Radius[mm] [3]’ can be set. If ‘Cylinder’ is selected, ‘Radius[mm] [3]’ and ‘Length[mm] [4]’ can be set.

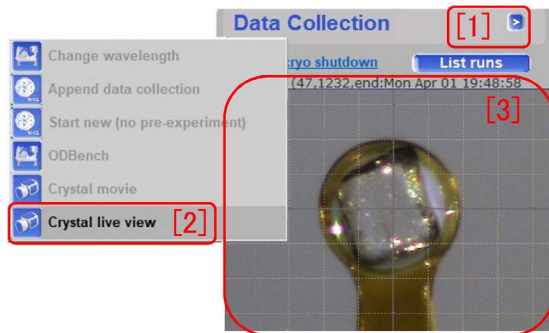


Figure 6.10: Crystal live view

#	t	start	end	width	exposure	speed/rat	omega	theta	kappa	phi	# to do	# done
1	o	-34.000	79.000	0.500	8.640	0.000	-	-10.200	28.000	-90.000	226	226
2	o	-100.000	79.000	0.500	8.640	0.000	-	-10.200	55.000	90.000	356	158
3	o	-100.000	-68.000	0.500	8.640	0.000	-	-10.200	55.000	30.000	68	0
4	o	-28.000	21.000	0.500	8.640	0.000	-	-10.200	55.000	30.000	98	0
5	o	-100.000	-71.000	0.500	8.640	0.000	-	-10.200	55.000	0.000	58	0
6	o	-100.000	-56.000	0.500	8.640	0.000	-	-10.200	55.000	-30.000	88	0
7	o	-100.000	43.000	0.500	8.640	0.000	-	-10.200	55.000	60.000	286	0
8	o	-98.000	-72.000	0.500	8.640	0.000	-	-10.200	28.000	-90.000	52	0

Figure 6.11: The main measurement schedule and status in progress

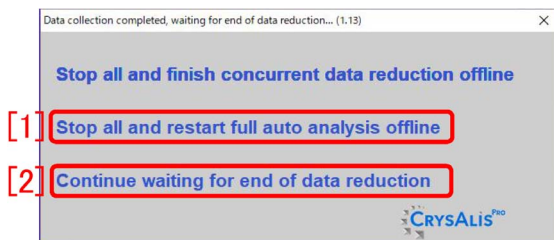


Figure 6.12: Menu shown after finishing the data collection

These settings are used when doing the empirical absorption correction. Settings can be finished by clicking Fig. 6.9 [p. 17] '[6] OK'.

In Fig. 6.10, '[1] >' can be clicked to display a menu on the left from which 'Crystal live view [2]' can be clicked to display real-time optical image of '[3]'.

In Fig. 6.11 '[2]' shows expected finish time. '[1] List runs' can be clicked to display a table in a red frame '[3]'. Here, '[4]' shows numbers of scheduled shots and '[5]' shows numbers of taken shots.

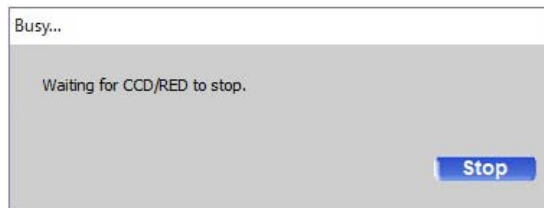


Figure 6.13: Message displayed during waiting the CCD stops

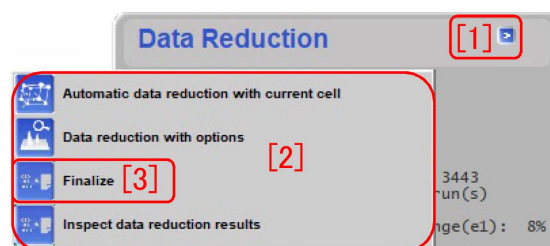


Figure 6.14: Menu of finalize

When the data collection is finished, Fig. 6.12 is displayed. If exchanging the crystal with the next one, '[1] Stop all and restart full analysis offline' should be clicked such as to let the off-line CrysAlis^{Pro} integrate the diffraction intensities that have been already measured and to prepare the next crystal. When Fig. 6.13 appeared, wait until the detector stops automatically, please.

'[1] >' on the right of Data Reduction tab in Fig. 6.14 can be clicked to open the menu of '[2]'. Here, 'Finalize [3]' can be clicked to open Fig. 6.15. Here, '[1] (Laue Group)' should be revised if it is wrong. '[2] Friedel mates:' should be non-equivalent when obtaining the absolute structure of the molecule by taking advantage of the bankruptcy of Friedel's law. The absolute structure is whether L-body or D-body (S-body or R-body) the molecule is. In the case of centrosymmetric crystals, '[2] Friedel mates:' should be clicked to be 'equivalent'. However, it should not be clicked to be 'non-equivalent' (recommended) when determining the chirality (absolute structure) of non-centrosymmetric molecule by taking advantage of the bankruptcy of Friedel's law. 'Numerical absorption [4] Faces' should be clicked when 3D data of the crystal shape have been obtained referring to the description in Appendix D [p.45].

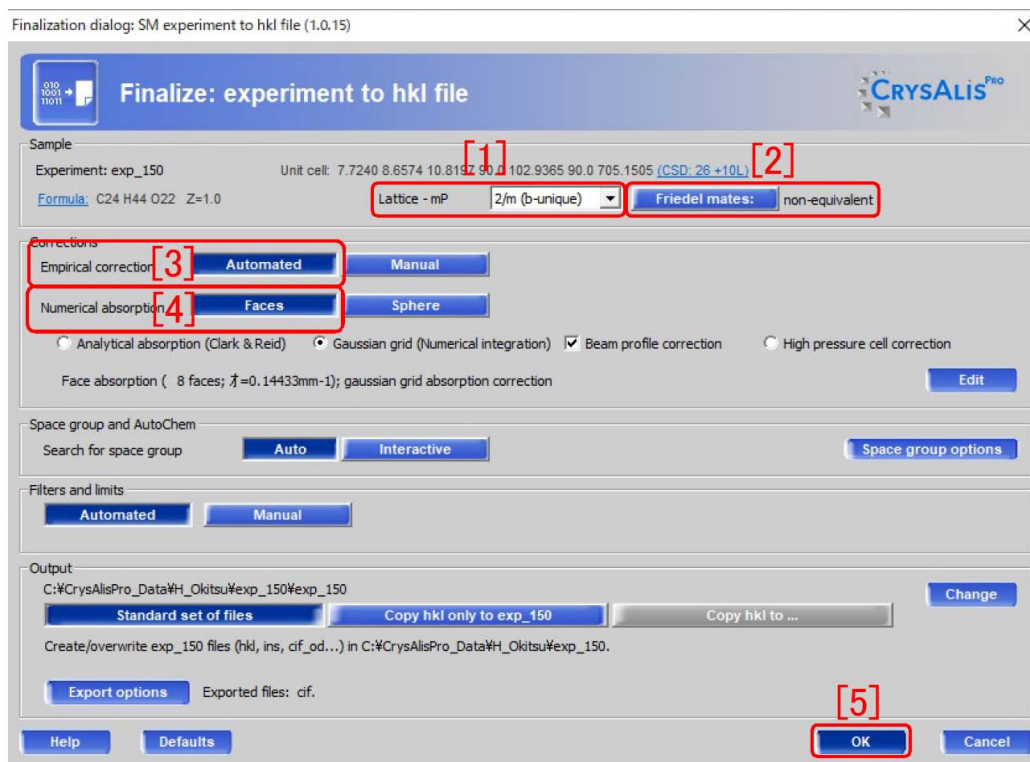


Figure 6.15: Finalize option



Figure 6.16: A message 'There is no photo of the crystal'

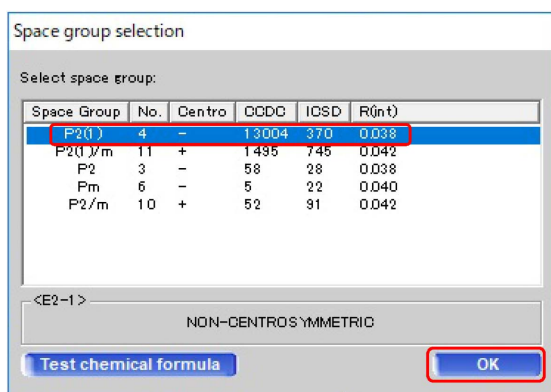


Figure 6.17: Selection of the space group

If 'Numerical absorption [4] Faces' is clicked without obtaining the 3D outline data, an alarm as shown in Fig. 6.16 is displayed. This button can be clicked again to continue. '[5] OK' in Fig. 6.15 can be clicked to close this window.

Fig. 6.17 is a list of feasible space groups. Here, it should be revised when it is wrong.

'[3] START/STOP' on the upper right of Fig. 0 on the cover of this manual and then '[4] Start new' on it should be clicked to go to the description of §3.1 [p.6]. Here, the new crystal can be mount to do the next experiment. The next measurement can be started by letting the off-line CrysAlis^{Pro} integrate the previous diffraction X-ray intensities. Even if the user does not have the next crystal, 'Mount' on the upper left of Fig. 3.2 [p.6] should be clicked to move the goniometer to the initial position.

6.5 Finishing the experiment

When finishing the experiment, '[2] Continue waiting for end of data reduction' in Fig. 6.12 should be clicked. In Fig. 6.18 [p.20], Status



Figure 6.18: Shutdown options

after finishing the experiment should be selected. If the next user does the experiment with the same X-ray source soon, '[1] Keep current generator settings' should be clicked. If the next user does not do the experiment soon or does it with the different X-ray source, '[2] Ramp generator down' should be clicked to display

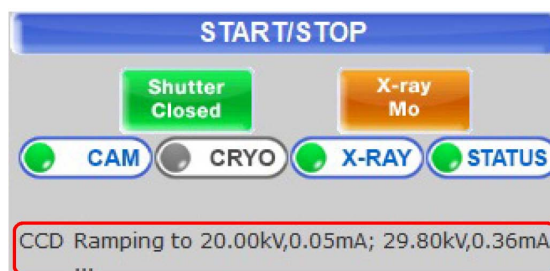


Figure 6.19: X-ray power is ramping down

Fig. 6.19. '[3] Turn generator off' to turn off the X-ray power soon, should not be clicked. '[4] Cancel' can be clicked to cancel the shutdown procedure.

Before removing the crystal from the goniometer head, '[4] Detector cover' in Fig. 3.6 [p.7] should necessarily be put such that **the detector surface is not touched**.

To be continued

Appendix A

Reasonability of defining the reciprocal lattice

For many students working on crystallography, the first difficulty is understanding of reciprocal lattice. In spite that the Bragg condition written by (A.1) or (A.2) can easily be understood, why such strange ideas as reciprocal lattice and reciprocal space should we use? This chapter describes the equivalence of Bragg's reflection condition, Laue's reflection condition and Ewald construction (Reciprocal lattice node exists on the Ewald sphere), from which how reasonably the reciprocal lattice is defined can be understood.

Every space group of crystal has an extinction rule owing to its symmetry with which the crystal structure factor comes to be zero. However, it is neglected in the following description for simplicity.

A.1 Bragg's reflection condition

Figure A.1 shows Bragg's reflection condition. This figure is also found in high school text book. Bragg's reflection condition can relatively easily and intuitively referring to this figure. When atoms (or molecules) are arranged on a set of planes as shown in Fig. A.1. Optical path length of X-rays drawn as a gray line are longer than that drawn as a black line by $|\vec{ab}| + |\vec{bc}| (= 2d \sin \theta_B)$. When this length is an integral multiplication of the wavelength, these rays interfere constructively with each other. Therefore, reflection condition can be described as follows,

$$2d \sin \theta_B = n\lambda. \quad (\text{A.1})$$

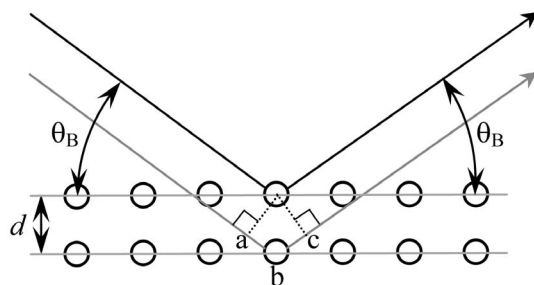


Figure A.1: Bragg's reflection condition.

By redefining lattice spacing d' to be $d' = d/n$, the following equation is also frequently used,

$$2d' \sin \theta_B = \lambda. \quad (\text{A.2})$$

Now, let us consider why the angle of incidence and emergence is identical. Is it evident since the Bragg plane works as a mirror plane? Then, why are the angles of incidence and emergence of a mirror identical? Sometimes, even a veteran of crystallography cannot answer to this question.

A.2 Laue's reflection condition

Laue's reflection condition was used to explain the phenomenon of X-ray diffraction when it was invented by Laue (Max Theodor Felix von Laue; 1879/10/9-1960/4/24) in 1912, which is described referring to Fig. A.2 as follows,

$$\begin{aligned} R_0B - AR_1 \\ = \overrightarrow{R_0R_1} \cdot \mathbf{s}_1 - \overrightarrow{R_0R_1} \cdot \mathbf{s}_0 = n_0\lambda. \end{aligned} \quad (\text{A.3})$$

Here, \mathbf{s}_0 and \mathbf{s}_1 are unit vectors in the direction of propagation of incident and reflected X-rays.

When R_0 and R_1 are equivalent lattice points, difference in optical path length between black and gray paths drawn in Fig. A.2 is given by (A.3). When this difference in path length is an integral multiplication of wavelength, X-rays scattered by lattice points R_0 and R_1 interfere constructively with each other.

Incidentally, since R_0 and R_1 are equivalent lattice point, there is a restriction as follows,

$$\overrightarrow{R_0R_1} = n_1\mathbf{a} + n_2\mathbf{b} + n_3\mathbf{c}, \quad (\text{A.4})$$

where, n_1 , n_2 and n_3 are arbitrary integers. \mathbf{a} , \mathbf{b} and \mathbf{c} are primitive translation vectors. That is to say the left hand side of (A.3) should be integral multiplication of wavelength for arbitrary integers n_1 , n_2 and n_3 . Lattice points R_0 and R_1 can move freely with a restriction that these are equivalent points. The value of left hand side of (A.3) is evidently positive when $\overrightarrow{R_0R_1} \cdot \mathbf{s}_1 > \overrightarrow{R_0R_1} \cdot \mathbf{s}_0$ and is negative when $\overrightarrow{R_0R_1} \cdot \mathbf{s}_1 < \overrightarrow{R_0R_1} \cdot \mathbf{s}_0$. Figure A.2 is drawn under an assumption of the latter case.

However, R_0 and R_1 can also be taken such that $\overrightarrow{R_0R_1} \cdot \mathbf{s}_1 = \overrightarrow{R_0R_1} \cdot \mathbf{s}_0$. In the following discussion in this paragraph, R_0 and R_1 are fixed such that $\overrightarrow{R_0R_1} \cdot \mathbf{s}_1 = \overrightarrow{R_0R_1} \cdot \mathbf{s}_0$. When R_0 , R_1 and optical paths drawn as black and gray lines are all on the drawing, there should be a plane perpendicular to the drawing that include those points and optical paths. When X-rays are scattered at any point on this plane under a condition that the angles of incidence and emergence are the same, the optical path length is always the same. This is also the reason for that the angle of incidence and emergence for a mirror is always identical.

In Bragg's reflection condition, under an implicit (the first and second dimensional) restriction that optical path length are always the same for a defined Bragg plane when the angle of incidence and emergence is identical, the third dimensional condition is given by (A.1) or (A.2). Behind the simple condition given by those equations, the above mentioned first and second dimensional restrictions are hidden.

Now, for description in the next section, the following equation is prepared by dividing the both sides of eq. (A.3) by the wavelength λ ,

$$\overrightarrow{R_0R_1} \cdot \left(\frac{\mathbf{s}_1}{\lambda} - \frac{\mathbf{s}_0}{\lambda} \right) = n_0. \quad (\text{A.5})$$

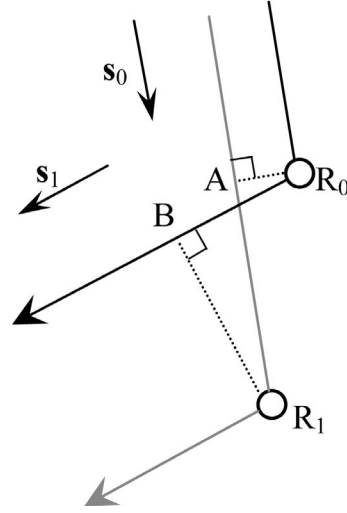


Figure A.2: Laue's reflection condition.

By substituting (A.4) into the above equation and considering that the wave vectors of incident and reflected X-rays are given by $\mathbf{K}_0 = \mathbf{s}_0/\lambda$ and $\mathbf{K}_1 = \mathbf{s}_1/\lambda$, the following equation can be obtained,

$$(n_1\mathbf{a} + n_2\mathbf{b} + n_3\mathbf{c}) \cdot (\mathbf{K}_1 - \mathbf{K}_0) = n_0. \quad (\text{A.6})$$

A.3 Ewald's reflection condition (Ewald construction)

A.3.1 Foundation of Ewald construction

Fig. A.3 [p.24] shows the situation that the origin O of reciprocal space and a reciprocal lattice node H_{hkl} simultaneously exist on the surface of Ewald sphere. Its center is the common initial point of wave vectors \mathbf{K}_0 and \mathbf{K}_1 .

In the description of Ewald construction, at first, reciprocal fundamental vectors \mathbf{a}^* , \mathbf{b}^* and \mathbf{c}^* are defined as follows:

$$\mathbf{a}^* = \frac{\mathbf{b} \times \mathbf{c}}{\mathbf{a} \cdot (\mathbf{b} \times \mathbf{c})}, \quad (\text{A.7a})$$

$$\mathbf{b}^* = \frac{\mathbf{c} \times \mathbf{a}}{\mathbf{a} \cdot (\mathbf{b} \times \mathbf{c})}, \quad (\text{A.7b})$$

$$\mathbf{c}^* = \frac{\mathbf{a} \times \mathbf{b}}{\mathbf{a} \cdot (\mathbf{b} \times \mathbf{c})}. \quad (\text{A.7c})$$

The denominator of (A.7), $\mathbf{a} \cdot (\mathbf{b} \times \mathbf{c})$ [= $\mathbf{b} \cdot (\mathbf{c} \times \mathbf{a}) = \mathbf{c} \cdot (\mathbf{a} \times \mathbf{b})$] is the volume of parallelepiped whose edges are \mathbf{a} , \mathbf{b} and \mathbf{c} . From

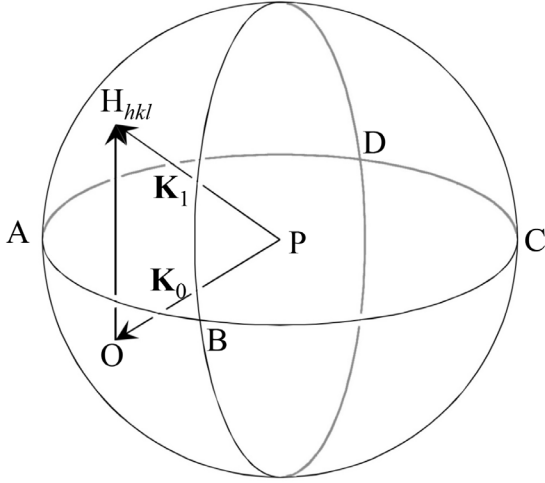


Figure A.3: Ewald sphere

the above definitions, the following equations are evident,

$$\mathbf{a} \cdot \mathbf{a}^* = 1, \quad (\text{A.8a})$$

$$\mathbf{b} \cdot \mathbf{b}^* = 1, \quad (\text{A.8b})$$

$$\mathbf{c} \cdot \mathbf{c}^* = 1. \quad (\text{A.8c})$$

Further, $\mathbf{b} \times \mathbf{c}$ is a vector that is perpendicular to both \mathbf{b} and \mathbf{c} and has a length of the area of parallelogram whose sides are \mathbf{b} and \mathbf{c} . Here, vectors \mathbf{b} , \mathbf{c} and $\mathbf{b} \times \mathbf{c}$ construct a right-handed system. Since the above is the same for $\mathbf{c} \times \mathbf{a}$ and $\mathbf{a} \times \mathbf{b}$, the following relations are also evident,

$$\mathbf{a} \cdot \mathbf{b}^* = \mathbf{a} \cdot \mathbf{c}^* = 0, \quad (\text{A.9a})$$

$$\mathbf{b} \cdot \mathbf{c}^* = \mathbf{b} \cdot \mathbf{a}^* = 0, \quad (\text{A.9b})$$

$$\mathbf{c} \cdot \mathbf{a}^* = \mathbf{c} \cdot \mathbf{b}^* = 0. \quad (\text{A.9c})$$

That is to say, \mathbf{a}^* , \mathbf{b}^* and \mathbf{c}^* have been defined such that (A.8) and (A.9) are satisfied.

A reflection vector giving $h k l$ reflection is defined in general as follows:

$$\overrightarrow{\text{OH}}_{hkl} = h\mathbf{a}^* + k\mathbf{b}^* + l\mathbf{c}^*. \quad (\text{A.10})$$

Here, O is the origin of reciprocal space. The Ewald sphere is a sphere whose center is P. The wave vector of the incident X-rays \mathbf{K}_0 is $\overrightarrow{\text{PO}}$. When a reciprocal lattice node H_{hkl} exists on the surface of the Ewald sphere, reflected X-rays whose wave vector \mathbf{K}_1 is $\overrightarrow{\text{OH}}_{hkl}$ are excited. Then, the following equation is satisfied,

$$\begin{aligned} \mathbf{K}_1 - \mathbf{K}_0 &= \overrightarrow{\text{OH}}_{hkl} \\ &= h\mathbf{a}^* + k\mathbf{b}^* + l\mathbf{c}^*. \end{aligned} \quad (\text{A.11})$$

Let us calculate the left-hand side of (A.6) [p.23] by substituting (A.11) into the second term of the left-hand side of (A.6) [p.23] and considering (A.8) and (A.9) as follows:

$$\begin{aligned} (n_x\mathbf{a} + n_y\mathbf{b} + n_z\mathbf{c}) \cdot (\mathbf{K}_1 - \mathbf{K}_0) \\ = (n_x\mathbf{a} + n_y\mathbf{b} + n_z\mathbf{c}) \cdot (h\mathbf{a}^* + k\mathbf{b}^* + l\mathbf{c}^*) \end{aligned} \quad (\text{A.12})$$

$$= n_x h + n_y k + n_z l. \quad (\text{A.13})$$

Since $n_x h + n_y k + n_z l$ is evidently an integer, Laue's reflection condition described by (A.3) [p.22], (A.5) [p.23] and (A.6) [p.23], is satisfied when the reciprocal lattice node H_{hkl} is on the surface of Ewald sphere. Therefore, Ewald's reflection condition is equivalent to Laue's reflection condition. Furthermore, Ewald's reflection condition is also equivalent to Bragg's reflection conditions, which is more clarified by the description in the next section A.3.2

Bragg's reflection condition can easily be understood by referring to Fig. A.1 [p.22]. Laue's reflection condition is more difficult than Bragg's reflection condition. However, it can also be understood by referring to Fig. A.2 [p.23]. The drawing of Fig. A.3 in reciprocal space was invented by Ewald. This way of drawing is extremely effective when considering various difficult problems in crystallography that cannot be understood by drawing figures as shown in Fig. A.1 [p.22] and /or Fig. A.2 [p.23] in real space. It is strongly recommended to use the Ewald construction by using Fig. A.3 by paying respect to Ewald (Paul Peter Ewald, 1888/1/23~1985/8/22).

A.3.2 Relation between reciprocal lattice vector and Bragg reflection plane

Reciprocal lattice vector is a vector whose direction is perpendicular to the Bragg plane and length is $1/d'$, where d' is the lattice spacing of the Bragg plane. These are verified in the following paragraphs.

By considering $n_0 = n_x h + n_y k + n_z l$, (A.10) and (A.12)=(A.13), the following equation is obtained.

$$\overrightarrow{\text{OH}}_{hkl} \cdot (n_x\mathbf{a} + n_y\mathbf{b} + n_z\mathbf{c}) = n_0. \quad (\text{A.14})$$

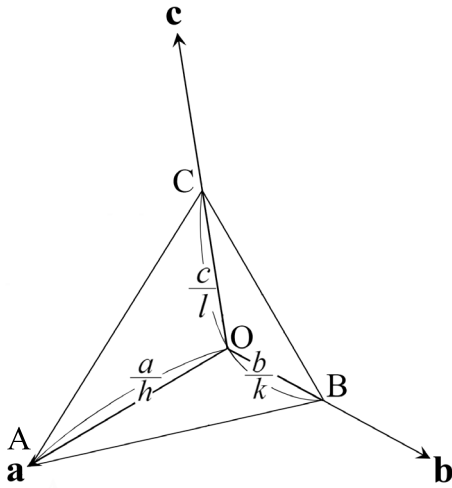


Figure A.4: Drawing of Miller and Miller indices

By multiplying $1/|\overrightarrow{OH_{hkl}}|$ to the both sides of the above equation, the following equation is obtained,

$$\frac{\overrightarrow{OH_{hkl}}}{|\overrightarrow{OH_{hkl}}|} \cdot (n_x \mathbf{a} + n_y \mathbf{b} + n_z \mathbf{c}) = \frac{n_0}{|\overrightarrow{OH_{hkl}}|}. \quad (\text{A.15})$$

A plane is described in general as follows:

$$\begin{aligned} & [\text{Unit normal vector}] \cdot [\text{Location vector}] \\ & = [\text{Distance from the origin}]. \end{aligned} \quad (\text{A.16})$$

Therefore, $n_0 \in \{ \dots, -2, -1, 0, 1, 2, \dots \}$ in (A.15) means that location vector $n_x \mathbf{a} + n_y \mathbf{b} + n_z \mathbf{c}$ is on Bragg planes piled up with a spacing of $d' (= 1/|\overrightarrow{OH_{hkl}}|)$, which reveals that the reciprocal lattice vector $\overrightarrow{OH_{hkl}}$ is the normal vector of Bragg plane whose length is $1/d'$.

A.4 Drawing of Miller and Miller indices

Fig. A.4 shows the relation between the Miller indices and the Bragg plane and is found in almost all text books describing the crystallography. This way of drawing was invented by Miller (William Hallows Miller; 1801/4/6-1880/5/20). However, it should be noted that

he was a mineralogist of the 19th century before X-rays and X-ray diffraction were invented. Figs. A.1[p.22] and A.4 are found in many text books. However, it cannot be recommended that the students and researchers attempt to understand the X-ray diffraction phenomena only by referring to Figs. A.1[p.22] and A.4.

Points A, B and C in Fig. A.4 exist on \mathbf{a} , \mathbf{b} and \mathbf{c} axes, respectively. Distances of them from the origin O are a/h , b/k and c/l . Miller invented that \mathbf{a} , \mathbf{b} and \mathbf{c} axes can be defined such that all facets of crystals are drawn as shown in Fig. A.4 with small integers h , k and l .

When $h = 0$, distance of A from O is infinite and then the plane ABC is parallel to \mathbf{a} . This is the case for k , B and \mathbf{b} and for l , C and \mathbf{c} .

h , k and l are indices of reciprocal lattice nodes, which was clarified several decades after Miller's invention. ABC is a plane whose direction is parallel to the Bragg plane and distance from O is d' . These are confirmed in the following description.

By referring to Fig. A.4, $\overrightarrow{AB} = -\mathbf{a}/h + \mathbf{b}/k$ and then $\overrightarrow{AB} \cdot \overrightarrow{OH_{hkl}}$ is calculated as follows:

$$\begin{aligned} \overrightarrow{AB} \cdot \overrightarrow{OH_{hkl}} &= (-\mathbf{a}/h + \mathbf{b}/k) \cdot (h\mathbf{a}^* + k\mathbf{b}^* + l\mathbf{c}^*) \\ &= -1 + 1 \\ &= 0. \end{aligned} \quad (\text{A.17})$$

Therefore, line AB is confirmed to be perpendicular to $\overrightarrow{OH_{hkl}}$. Similarly, lines BC and CA are confirmed to be perpendicular to $\overrightarrow{OH_{hkl}}$. Further, from this, the distance of ABC from the origin O can be obtained from scalar product between the unit normal vector of plane ABC and vector \overrightarrow{OA} , \overrightarrow{OB} or \overrightarrow{OC} as follows:

$$\begin{aligned} & \overrightarrow{OA} \cdot \overrightarrow{OH_{hkl}} / |\overrightarrow{OH_{hkl}}| \\ &= \frac{\mathbf{a}}{h} (h\mathbf{a}^* + k\mathbf{b}^* + l\mathbf{c}^*) / |\overrightarrow{OH_{hkl}}| \\ &= 1 / |\overrightarrow{OH_{hkl}}| \\ &= d' \end{aligned} \quad (\text{A.18})$$

As described above, the explanation of Fig. A.4 needs complex descriptions. It cannot be recommended to understand the phenomena of X-ray diffraction only referring to the drawing of Miller as shown in Fig. A.4.

Appendix B

Determination of space group from extinction rule

==> general reflections sorted into even/odd parity classes

eee			eoo			ooo		
totl	obsd	<I/sig>	totl	obsd	<I/sig>	totl	obsd	<I/sig>
205	196	30.0	[1] 253	240	29.2	289	272	32.1
eoo			oeo			ooo		
370	354	38.4	337	322	40.5	419	392	40.3
ooo			ooo↓					
318	297	33.6	355	343	38.6			

==> Special reflections sorted into various classes
 A * indicates a potential systematic absence and is used if the average I/sig(I) for a particular class is less than 3.5.

ee			eo			
totl	obsd	<I/sig>	totl	obsd	<I/sig>	
hhl refl	27	24	48.5	36	35	58.0
h-hl refl	30	28	49.2	37	35	55.7
OkI zone	89	80	43.2	110	106	54.0
h0l zone	34	31	43.8	40	11	2.2*
hk0 zone	62	57	39.1	68	65	53.8

oe			oo			
totl	obsd	<I/sig>	totl	obsd	<I/sig>	
hhl refl	40	39	45.4	47	44	68.4
h-hl refl	40	38	48.0	44	40	66.9
OkI zone	97	94	53.9	109	103	48.9
h0l zone	36	36	73.1	43	13	2.5*
hk0 zone	71	64	46.7	74	72	46.5

e			o			
totl	obsd	<I/sig>	totl	obsd	<I/sig>	% of o/e
hhh line	2	2	31.3	7	5	71.6
hh0 zone	7	7	42.2	9	9	98.6
Ok0 line	17	17	74.6	16	2	1.7*
00l line	10	8	102.3	9	1	2.4*
h00 line	3	3	95.0	6	6	38.3

Figure B.1: Content of 'process.out' (#1). [Taurine; monoclinic $P2_1/c$ (#14)].

One of the most important process in the crystal structure analysis is determination of space group. CrystalStructure 4.1 determines the space group automatically as shown in Fig. B.3.

In this chapter, how the computer determines the space group, is described. When the computer failed to determine the space group correctly, it should be determined manually referring to the description of this chapter.

Figs. B.1, B.2 and B.3 show contents of 'process.out' displayed by clicking 'View output file' button in Fig. 2.12 of Part2a manual. In this file, information about the extinction rule based

==> reflections sorted for identifying 4n type conditions
 a and b represent h, k, or l

a+b=4n			a+b not equal 4n			
totl	obsd	<I/sig>	totl	obsd	<I/sig>	
OkI zone	106	102	49.6	299	281	50.1
h0l zone	37	20	18.2	116	71	30.8
hk0 zone	69	66	38.9	206	192	48.8

a=4n			a not equal 4n			
totl	obsd	<I/sig>	totl	obsd	<I/sig>	
Ok0 line	8	8	77.5	25	11	28.2
00l zone	4	2	60.2	15	7	54.3
h00 zone	1	1	91.3	8	8	41.4

2h+l=4n			2h+l not equal 4n			
totl	obsd	<I/sig>	totl	obsd	<I/sig>	
hkl refl	34	32	47.5	116	110	59.9

==> reflections sorted for identifying 3n and 6n type conditions

h+l=3n; l odd			h+l=3n			h+l not equal 3n			
totl	obsd	<I/sig>	totl	obsd	<I/sig>	totl	obsd	<I/sig>	
h-h0l	26	24	54.1	54	52	64.6	97	89	51.8

-h+l=3n; l even			-h+l=3n			-h+l not equal 3n			
totl	obsd	<I/sig>	totl	obsd	<I/sig>	totl	obsd	<I/sig>	
h-h0l	26	22	62.7	49	43	55.6	102	98	56.7

l=3n			l not equal 3n			
totl	obsd	<I/sig>	totl	obsd	<I/sig>	
000l line	7	2	32.5	12	7	67.7

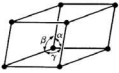
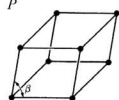
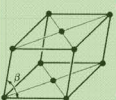
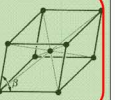
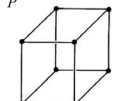
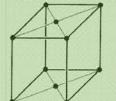
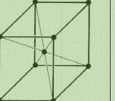
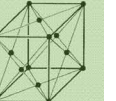
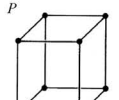
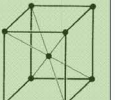
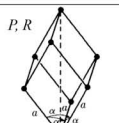
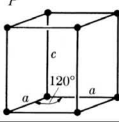
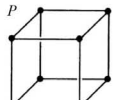
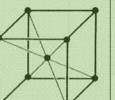

l=6n			l not equal 6n			
totl	obsd	<I/sig>	totl	obsd	<I/sig>	
000l line	2	2	185.7	17	7	47.2

Figure B.2: Content of 'process.out' (#2). [Taurine; monoclinic $P2_1/c$ (#14)]

on which the space group can be determined, are summarized.

Information about extinctions of reflections whose three, two or one indices are not zero, are summarized on parts [1], [2, 3] and [4], respectively, of Fig. B.1. For example, 'eoo' found on the upper part of [1] in Fig. B.1 means that indices of hkl are even, even and odd. 'totl' and 'obsd' are numbers of total and observed reflections. $\langle I/\sigma \rangle$ are mean values of I/σ , where I is observed intensity of reflected X-rays and σ is standard deviation of background. Since values of 'obsd' and $\langle I/\sigma \rangle$ are sufficiently large, there is no extinction for three nonzero hkl . On parts [2] and [3] in Fig. B.1, $h0l$ reflections are

Table B.1: 14 Bravais lattices and ‘Face-centered monoclinic’. Refer to the last paragraph of §B.2 [p.29], please about why ‘Face-centered monoclinic’ is added.

Crystal system Laue group (No. of space group)	Axial distances (a, b, c) Axial angles (α, β, γ)	Primitive lattice (P, R)	Base-centered lattice (A, B, C)	Body-centered lattice (I)	Face-centered lattice (F)
Triclinic $\bar{1}$ (#1, #2)	$a \neq b \neq c$ $\alpha \neq \beta \neq \gamma$				
Monoclinic $2/m$ (#3 ~#15)	$a \neq b \neq c$ two of α, β, γ $= 90^\circ$, one $\neq 90^\circ$				
Orthorhombic mmm (#16 ~#74)	$a \neq b \neq c$ $\alpha = \beta = \gamma$ $= 90^\circ$				
Tetragonal $4/m$ (#75 ~#88), $4/mmm$ (#89 ~#142)	Two of a, b, c are the same. One of them is different. $\alpha = \beta = \gamma$ $= 90^\circ$				
Trigonal $\bar{3}$ (#143 ~#148), $\bar{3}m$ (#149 ~#167)	$a = b = c$ $\alpha = \beta = \gamma$ $\neq 90^\circ$				
Hexagonal $6/m$ (#168 ~#176) $6/mmm$ (#177 ~#194)	a and b are the same. c is different. $\alpha = \beta = 90^\circ$ $\gamma = 120^\circ$				
Cubic $m\bar{3}$ (#195 ~#206) $m\bar{3}m$ (#207 ~#230)	$a = b = c$, $\alpha = \beta = \gamma$ $= 90^\circ$				

o/e' are extremely small. In parts [5] and [6] in

Space group # 14 setting # 1
The selected space group symbol is: $P2_1/c$

Figure B.3: Content of ‘process.out’ (#3) [Taurine; monoclinic $P2_1/c$ (#14)]. [setting #1] corresponds to ‘[1] CELL CHOICE 1’ in Fig. B.5.

recognized to distinguish since value of $\langle I/\text{sig} \rangle$ is extremely small when l is odd. This is indicated by an ‘*’ mark. Similarly, in part [4] in Fig. B.1, $0k0$ and $00l$ reflections are recognized to distinguish when k is odd and l is odd, respectively since values of $\langle I/\text{sig} \rangle$ and ‘% of

Reflection conditions

General:

$$h0l : l = 2n$$

$$0k0 : k = 2n$$

$$00l : l = 2n$$

Figure B.4: Reflection condition of $P2_1/c$ (#14) described in *International Tables for Crystallography* (2006) Vol.A. $0k0$ reflections when k is odd and, $h0l$ and $00l$ reflections when l is odd, extinguish.

Fig. B.2, information about reflection indices when indices or summation of them are

W. G. Wyckoff; 1897/8/9~1994/11/3)

Table B.2: Symmetric elements (planes). Protein crystals do not have these symmetric elements absolutely.

Name of symmetric plane	Symbol	Graphic symbol (perpendicular to the space)	Graphic symbol (parallel to the space)
Mirror plane	m		
Axial glide plane	a, b or c		
Axial glide plane	a, b or c		
Double glide plane	e		
Diagonal glide plane	n		
Diamond glide plane	d		

Table B.3: Symmetric elements of crystal (axes and point).

Symmetric axis or center	Symbol	Graphic symbol (perpendicular to the space)	Graphic symbol (parallel to the space)
-	1		
Two-fold rotation axis	2		
2_1 screw axis	2_1		
Three-fold rotation axis	3		
3_1 screw axis	3_1		
3_2 screw axis	3_2		
Four-fold rotation axis	4		
4_1 screw axis	4_1		
4_2 screw axis	4_2		
4_3 screw axis	4_3		
Six-fold rotation axis	6		
6_1 screw axis	6_1		
6_2 screw axis	6_2		
6_3 screw axis	6_3		
6_4 screw axis	6_4		
6_5 screw axis	6_5		
Symmetry center	$\bar{1}$		
Three-fold rotatory inversion axis	$\bar{3}$		
Four-fold rotatory inversion axis	$\bar{4}$		
Six-fold rotatory inversion axis	$\bar{6}$		

divided by 4, by 3 and by 6, from which existence of four-, three- and six-fold screw axes can be discussed.

Fig. B.3 [p.27] shows that the space group of taurine crystal has been determined to be $P2_1/c$ (#14).

Fig. B.4 shows reflection condition of $P2_1/c$ (#14) described in *International Tables for Crystallography* (2006) Vol.A. The information described in Figs. B.1 [p.26] and B.2 [p.26] coincides with the condition in Fig. B.4 [p.27], from which the space group has been determined to be $P2_1/c$ (#14).

In the following description, how the extinction of reflections are caused by symmetries of crystals depending on the space group, is explained.

B.1 Symmetric elements of crystal derived based on the group theory

Who showed the importance of group theory to determine the crystal structure for the first time was Shoji Nishikawa (1884/12/5~1952/1/5). Wyckoff (R.

who was strongly influenced by Nishikawa, systemized and established the space group theory that is widespread today and summarized in *International Tables for Crystallography* (2006) Vol.A.

As shown in Table B.1 [p.27], crystals are categorized into seven crystal systems depending on their shapes of unit cells. Further, there are several complex lattices whose backgrounds in Table B.1 [p.27] are green, other than primitive cells. Fourteen kinds of lattice except for ‘body-centered monoclinic lattice’ are called Bravais lattice.

‘Body-centered monoclinic lattice’ was added by the present author’s own judgment. The reason is that base-centered monoclinic lattice can sometimes change to body-centered lattice without changing the symmetry of monoclinic lattice or changing volume of unit cell by reselecting axes of unit cell.

In the first column of Table B.1 [p.27], Laue groups and ranges of space group number are summarized. Laue group is determined by symmetry of reciprocal lattice of crystals.

It has been clarified that crystals can be categorized into 230 space groups depending on the symmetric elements as shown in Tables. B.1 [p.27], B.2 and B.3.

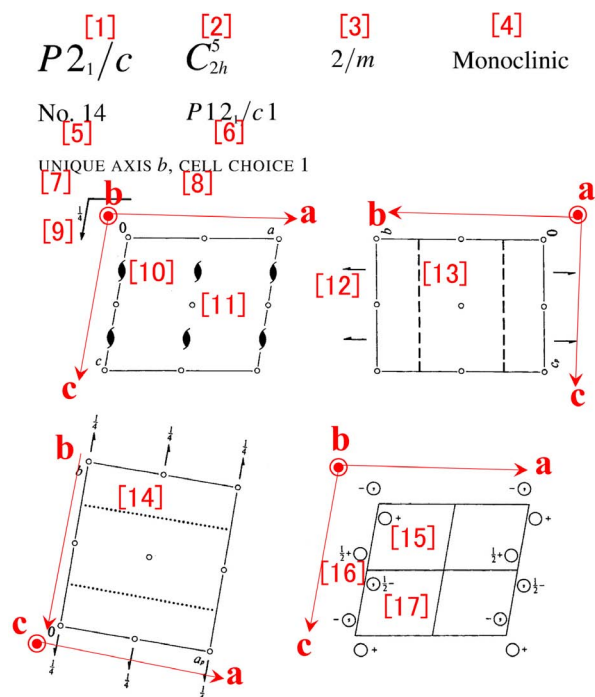


Figure B.5: Drawings for space group $P2_1/c$ (#14) in *International Tables for Crystallography* (2006) Vol.A. Protein crystals do not belong to this space group absolutely.

What is important to determine the space group is the extinction rule, about which the information can be extracted by referring to descriptions in ‘process.out’ as shown in Figs. B.1 [p.26] and B.2 [p.26]. It can be viewed by clicking ‘View output file’ button in Fig. 2.21 of Part 2a manual.

B.2 Symbols of space groups

Fig. B.5 is a diagram on the first two pages showing symmetric elements of crystal group $P12_1/c1$ in *International Tables for Crystallography* (2006) Vol.A, Chapter 7. Marks [1]-[17] are as follows; [1]: Hermann-Mouguin notation, [2]: Schönflies notation, [3]: Laue group, [4]: crystal system, [5]: ordinal number of space group, [6]: Hermann-Mouguin full notation, [7]: unique axis, [8]: cell choice, [9]: graphic symbol of c glide plane, [10]: graphic symbol of 2_1 screw axis, [11]: graphic symbol of symmetric center, [12]: graphic symbol of 2_1 screw axis, [13]: graphic symbol of c glide plane, [14]: graphic symbol of c glide plane, [15]: position

Table B.4: Extinctions owing to complex lattice.

Name of lattice	Symbol	Reflection condition(not extinct)	Example
A base-centered	A	$hkl : k + l = 2n$	$A 12/n1$ (#15)
B base-centered	B	$hkl : h + l = 2n$	$B 2/n11$ (#15)
C base-centered	C	$hkl : h + k = 2n$	$C 12/c1$ (#15)
Body-centered	I	$hkl : h + k + l = 2n$	$I 2/b11$ (#15)
Face-centered	F	$hkl : h + k, h + l, k + l = 2n$	

Table B.5: Extinction rules owing to glide planes. Protein crystals do not have glide plane absolutely.

Name of glide plane (Symbol)	Normal to	Reflection condition (not extinct)	Example
Axial glide plane (a)	\mathbf{b}	$h0l : h = 2n$	$P 12_1/a1$ (#14)
Axial glide plane (a)	\mathbf{c}	$hk0 : h = 2n$	$P 112_1/a$ (#14)
Axial glide plane (b)	\mathbf{a}	$0kl : k = 2n$	$P 2_1/b 11$ (#14)
Axial glide plane (b)	\mathbf{c}	$hk0 : k = 2n$	$P 112_1/b$ (#14)
Axial glide plane (c)	\mathbf{a}	$0kl : l = 2n$	$P 2_1/c11$ (#14)
Axial glide plane (c)	\mathbf{b}	$h0l : l = 2n$	$P 12_1/c1$ (#14) $C 12/c1$ (#15)
Double glide plane (e)	\mathbf{a}	$hkl : k + l = 2n$	
Double glide plane (e)	\mathbf{b}	$hkl : h + l = 2n$	
Double glide plane (e)	\mathbf{c}	$hkl : h + k = 2n$	
Diagonal glide plane (n)	\mathbf{a}	$0kl : k + l = 2n$	$B 2/n11$ (#15)
Diagonal glide plane (n)	\mathbf{b}	$h0l : h + l = 2n$	$C 12/c1$ (#15)
Diagonal glide plane (n)	\mathbf{c}	$hk0 : h + k = 2n$	$P 112_1/n$ (#14)

of atom, [16]: position of atom (an image due to 2_1 screw axis), [17]: position of atom (an image due to c glide plane).

‘[8] CELL CHOICE 1’ corresponds to ‘setting #1’ in Fig. B.3 [p.27]. ‘ $\frac{1}{4}$ ’ described near [9] is the height of c glide plane. About graphic symbols of c glide plane [9], [13] and [14], refer to Table B.2 [p.28], please. About graphic symbols of 2_1 screw axis [10] and [12], refer to Table B.3 [p.28]. Atoms at positions [16] and [17] are images of atom at [15] by symmetric operations due to 2_1 screw axis and c glide plane, respectively. ‘ $\frac{1}{2}+$ ’ near [16] and ‘ $\frac{1}{2}-$ ’ near [17] means that locations of atoms at [16] and [17] are $-xa + (\frac{1}{2} + y)\mathbf{b} + (\frac{1}{2} - z)\mathbf{c}$ and $xa + (\frac{1}{2} - y)\mathbf{b} + (\frac{1}{2} + z)\mathbf{c}$, respectively when that of [15] is $xa + y\mathbf{b} + z\mathbf{c}$. Comma (,) in ‘O’ at [17] means that this atom (or molecule) is an enantiomer of those at [15] and [16].

Initial character of Hermann-Mouguin notation is P (or R partially for trigonal system) for primitive lattice, A , B or C for base-centered lattice, I for body-centered lattice or F for face-centered lattice. In many cases of base-

Table B.6: Extinction owing to screw axes.

Name of screw axis	Direction	Reflection condition (not extinct)	Example
2 ₁ screw axis	a	$h00: h = 2n$	$P2_12_12_1$ (#19)
2 ₁ screw axis	b	$0k0: k = 2n$	$P12_11$ (#4)
			$P12_1/c1$ (#14)
			$C12/c1$ (#15)
			$P2_12_12_1$ (#19)
2 ₁ screw axis	c	$00l: l = 2n$	$P2_12_12_1$ (#19)
3 ₁ screw axis	c	$00l: l = 3n$	
3 ₂ screw axis	c	$00l: l = 3n$	
4 ₁ screw axis	c	$00l: l = 4n$	
4 ₂ screw axis	c	$00l: l = 2n$	
4 ₃ screw axis	c	$00l: l = 4n$	
6 ₁ screw axis	c	$00l: l = 6n$	
6 ₂ screw axis	c	$00l: l = 3n$	
6 ₃ screw axis	c	$00l: l = 2n$	
6 ₄ screw axis	c	$00l: l = 3n$	
6 ₅ screw axis	c	$00l: l = 6n$	

centered lattice, C is mainly used for H-M notations. However, there are four exceptions, i.e. $Amm2$ (#38), $Abm2$ (#39), $Ama2$ (#40) and $Aba2$ (#41).

There are nine H-M full notations, i.e. $P12_1/c1$, $P12_1/n1$, $P12_1/a1$, $P112_1/a$, $P112_1/n$, $P112_1/b$, $P2_1/b11$, $P2_1/n11$, $P2_1/c11$ for $P2_1/c$ due to arbitrariness to take axes. There are plural H-M full notations for an H-M notation in general. In some cases, however, there is only one H-M full notation, e.g. $P2_12_12_1$ (orthorhombic #19) since it has an identical symmetric element all in the directions of a , b and c axes.

In the case of $C2/c$, one of H-M full notation is $I12/a1$ when changing the choice of unit cell axes. This is the reason for ‘body-centered monoclinic lattice’ is added in Table B.1 [p.27].

B.3 How to read extinction rules

In this section, how to determine the space group by reading ‘process.out’ as shown in Figs. B.1 [p.26] and B.2 [p.26] and comparing them with *International Tables for Crystallography* (2006) Vol.A, Chapter 3.1, is described. When the space group were determined not correctly, it should be redetermined referring to the fol-

Table B.7: *International Tables for Crystallography* (2006) Vol.A, A part of *International Tables for Crystallography* (2006) Vol.A, Chapter 3.1.

MONOCLINIC, Laue class $2/m$

Unique axis b				Laue class $1\ 2/m\ 1$		
Reflection condition				Point group		
hkl	$h0l$	$0k0$	Extinction symbol	2	m	$2/m$
$0kl\ hk0$	$h00\ 00l$	$0k0$	$P1-1$	$P121$ (3)	$P1m1$ (6)	$P1\ 2/m\ 1$ (10)
		k	$P12_11$	$P12_11$ (4)		$P1\ 2_1/m\ 1$ (11)
			$P1a1$		$P1a1$ (7)	$P1\ 2/a\ 1$ (13)
[1]	h	k	$P1\ 2_1/a\ 1$			$P1\ 2_1/a\ 1$ (14)
	l		$P1c1$		$P1c1$ (7)	$P1\ 2/c\ 1$ (13)
[2]	l	k	$P1\ 2_1/c\ 1$			$P1\ 2_1/c\ 1$ (14)
	$h+l$		$P1n1$		$P1n1$ (7)	$P1\ 2/n\ 1$ (13)
[3]	$h+l$	k	$P1\ 2_1/n\ 1$			$P1\ 2_1/n\ 1$ (14)
$h+k$	h	k	$C1-1$	$C121$ (5)	$C1m1$ (8)	$C1\ 2/m\ 1$ (12)
$h+k$	h, l	k	$C1c1$		$C1c1$ (9)	$C1\ 2/c\ 1$ (15)
$k+l$	l	k	$A1-1$	$A121$ (5)	$A1m1$ (8)	$A1\ 2/m\ 1$ (12)
$k+l$	h, l	k	$A1n1$		$A1n1$ (9)	$A1\ 2/n\ 1$ (15)
$h+k+l$	$h+l$	k	$I1-1$	$I121$ (5)	$I1m1$ (8)	$I1\ 2/m\ 1$ (12)
$h+k+l$	h, l	k	$I1a1$		$I1a1$ (9)	$I1\ 2/a\ 1$ (15)

lowing description.

Table B.7 shows a part of *International Tables for Crystallography* (2006) Vol.A, Chapter 3.1. Here, relations between the extinction rule and space group, are summarized. You can refer to pdf version of *International Tables for Crystallography* (2006) Vol.A, Chapter 3.1 that is placed on the desktop of computers.

In part [1] of Fig. B.1 [p.26] reflection conditions for hkl all of which are not zero, is described. Since no extinction can be found, the first column of Table B.7 should be empty. $h+k$, $k+l$ and $h+k+l$ in this column means that reflection indices that satisfies $h+k = 2n$, $k+l = 2n$ and $h+k+l = 2n$ do not distinguish. In first, second and third column in Table B.7, ‘= 2n’ is omitted.

In the case of Fig. B.1 [p.26], $0k0$ and $00l$ reflections distinguish when k is odd and when l is odd, respectively, which corresponds to [1], [2] and [3] rows in Table B.7. Therefore, H-M full notation of the space group of taurine is $P12_1/a1$, $P12_1/c1$ or $P12_1/n1$. These all belong to $P2_1/c$ (#14).

For redesignating space group in Crystal-Structure 4.1, ‘Space Group’ Menu window as shown in Fig. B.6 [p.31] can be opened by clicking ‘Space Group’ from ‘Parameters’ menu. Since b axis is usually taken as the main axis in the case of monoclinic crystal system, $P12_1/c1$

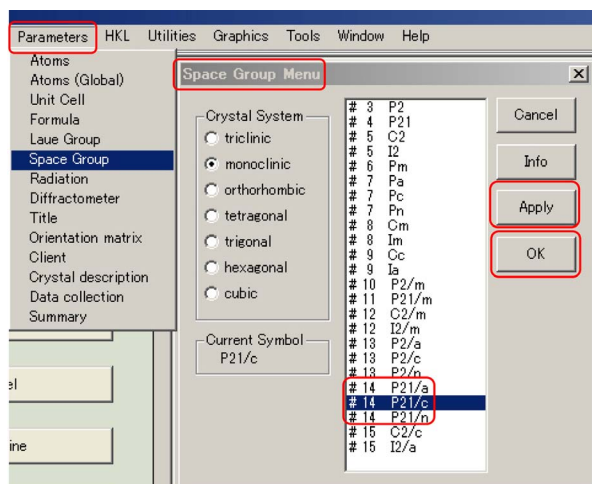


Figure B.6: Redesignation of space group in CrystalStructure 4.1. (in the case of small molecular-weight crystal).

should be selected. Then, click ‘Apply’ and ‘OK’ in this order, please.

B.4 Examples of extinction rules due to combinations of symmetric elements

In this section, several examples are described, in which the extinction rules are given by combinations of symmetric elements as summarized in Tables B.4 [p.29], B.5 [p.29] and B.6.

In cases of small molecular-weight organic crystals, frequently found space groups can be listed up in order of decreasing as follows, $P2_1/c$ (#14), $P\bar{1}$ (#2), $C2/c$ (#15), $P2_12_12_1$ (#19), $P2_1$ (#4). As many as 80% of small molecular weight organic crystals are occupied by those with space groups that belong to the above five.

In the cases of protein crystals, however, Hermann-Morguin notations of their space group do not have symbols of $\bar{1}$ (symmetric center), m (mirror plane), a , b , c , d , e and n (glide planes) absolutely since they need both optical enantiomer molecules in spite that protein molecules consist of only L amino acids but not of D amino acids. (L and D amino acids are optical enantiomer with each other). Also in the cases of small molecular-weight crystals, when they consist of chiral

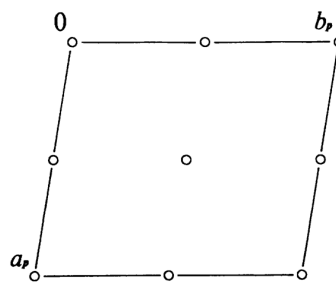


Figure B.7: Drawing for $P\bar{1}$ (#2) in *International Tables for Crystallography* (2006) Vol.A. Since this space group has symmetric center, protein crystals do not belong to it. The phase problem is simple (0 or π (180°)).

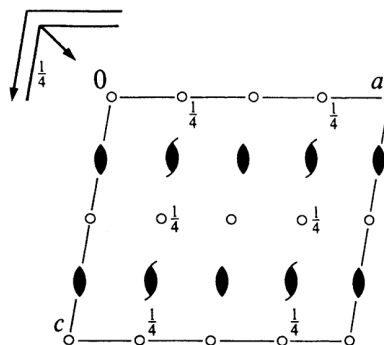


Figure B.8: Drawing for $C12/c1[C2/c]$ (#15) in *International Tables for Crystallography* (2006) Vol.A. Protein crystals do not belong to this space group absolutely since it has glide plane.

molecules, H-M notations of them do not have $\bar{1}$, m , a , b , c , d , e and n . In the cases of racemic crystals, these symbols are frequently included in their H-M notations.

Read the following description, please by referring Tables B.4 [p.29], B.5 [p.29] and B.6.

It can be read from Fig. B.5 [p.29] that space group $P2_1/c$ ($P12_1/c1$) has c glide plane and 2_1 screw axis in the direction of b . Reflection conditions due to these symmetric elements can be read from Tables B.5 [p.29] and B.6.

Reflection conditions are described in *International Tables for Crystallography* (2006) Vol.A dividing three cases in which one, two and three indices of hkl are not zero. Following this rule, the reflection conditions due to

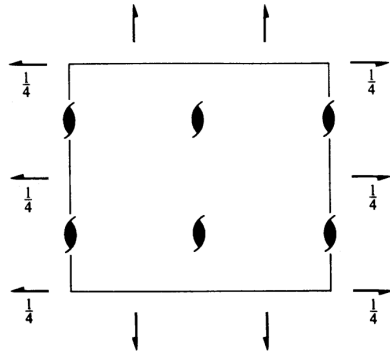


Figure B.9: *International Tables for Crystallography* (2006) Vol.A $P2_12_12_1$ (#19).

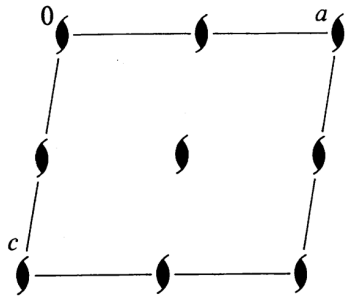


Figure B.10: *International Tables for Crystallography* (2006) Vol.A $P12_11$ [$P2_1$](#4).

c glide plane and 2_1 screw axis are described as follows,

$$\begin{aligned} h0l : & \quad l = 2n, \\ 0k0 : & \quad k = 2n, \\ 00l : & \quad l = 2n. \end{aligned}$$

This is found as shown in Fig. B.4 [p.27] in *International Tables for Crystallography* (2006) Vol.A.

Symmetric element that space group $P\bar{1}$ (#2) has, is only symmetric center. Therefore, there is no extinction. Protein crystals and chiral crystals do not belong to this space group, absolutely.

However, the phase problem is extremely simple (0 or π (180°)). Therefore, the molecular structure can be obtained frequently even for a crystal with low quality.

Since the initial character of $C12/c1$ is C , it is base-centered lattice. Since there are symmetric centers indicated by small open circles, the phase problem is very simple (0 or π (180°)).

Then, the molecular structure can be solved with high possibility.

Due to arbitrariness to take axes, there are three kinds of base-centered lattice, i.e. A base-centered, B base-centered and C base-centered lattice. However, let us focus the discussion on C base-centered lattice, here. The reflection condition shown in Table B.4 [p.29] can be written down dividing it into three cases in which one, two and three indices are not zero, as follows, $[hkl : h + k = 2n]$, $[hk0 : h + k = 2n]$, $[h0l : h = 2n]$, $[0kl : k = 2n]$, $[h00 : h = 2n]$, $[0k0 : k = 2n]$.

Referring to Fig. B.8[p.31], we can understand the existence of c glide plane, n glide plane and 2_1 screw axis that are perpendicular to \mathbf{b} axis. The reflection condition due to c glide plane and n glide plane perpendicular to b axis can be read to be $[h0l : h, l = 2n]$. Further, that due to 2_1 screw axis can be read to be $[0k0 : k = 2n]$.

The logical product of the above conditions can be written down as follows,

$$\begin{aligned} hkl : & \quad h + k = 2n, \\ h0l : & \quad h, l = 2n, \\ 0kl : & \quad k = 2n, \\ hk0 : & \quad h + k = 2n, \\ 0k0 : & \quad k = 2n, \\ h00 : & \quad h = 2n, \\ 00l : & \quad l = 2n. \end{aligned}$$

B.4.1 Orthorhombic $P2_12_12_1$ (#19)

It is evident from Fig. B.9 that $P2_12_12_1$ (#19) has 2_1 screw axes all in the directions of a , b and c axes. Therefore, referring to Table B.6 [p.30], the reflection condition is given as follows,

$$\begin{aligned} h00 : & \quad h = 2n, \\ 0k0 : & \quad k = 2n, \\ 00l : & \quad l = 2n. \end{aligned}$$

B.4.2 Monoclinic $P12_11$ [$P2_1$](#4)

There are three H-M full notations for space group $P2_1$ (#4). Here, the description is given for $P12_11$.

Space group $P12_11$ has 2_1 screw axis as shown in Fig. B.10. Therefore, as described in Table

B.6 [p.30], it has a reflection condition as follows,

$$0k0 : k = 2n.$$

B.5 Mathematical proofs of extinction rules

When the reader has time, refer to this chapter, please.

The extinction of reflection is caused by the existence of complex latticeC glide plane and screw axis whose background color is green in Tables B.1[p.27], B.2[p.28] and B.3[p.28]. To the contrary, only the above three symmetric elements give the extinction. However, protein crystals do not have glide plane absolutely. In this chapter, mathematical proofs of extinction due to the above symmetric elements are described.

For later description, let us note the definition of crystal structure factor, F_{hkl} for hkl reflection given as follows,

$$\begin{aligned} F_{hkl} &= \int_{\text{cell}} \rho(\mathbf{r}) \exp[-i2\pi(\mathbf{h} \cdot \mathbf{r})] dv. \\ &= \int_{\text{cell}} \rho(\mathbf{r}) \exp[-i2\pi(hx + ky + lz)] dv. \end{aligned} \quad (\text{B.1})$$

Here, $\int_{\text{cell}} dv$ is a volume integral over a unit cell, $\rho(\mathbf{r})$ is electron density at location \mathbf{r} ($= x\mathbf{a} + y\mathbf{b} + z\mathbf{c}$), and \mathbf{h} ($= h\mathbf{a}^* + k\mathbf{b}^* + l\mathbf{c}^*$) is a reciprocal lattice vector giving $h k l$ reflection. With regard to reciprocal lattice, refer to Appendix A [p.22], please.

Symmetry element that makes N equivalent points can be described as follows,

$$\rho[T^{(i)}(\mathbf{r})] = \rho[T^{(0)}(\mathbf{r})], \quad i \in \{0, 1, \dots, N-1\}.$$

Since F_{hkl} is zero when the N integral elements,

$$\sum_{i=0}^{N-1} \rho[T^{(0)}(\mathbf{r})] \exp[-i2\pi\mathbf{h} \cdot T^{(i)}(\mathbf{r})] = 0$$

That is to say,

$$\sum_{i=0}^{N-1} \exp[-i2\pi\mathbf{h} \cdot T^{(i)}(\mathbf{r})] = 0 \quad (\text{B.2})$$

B.5.1 Extinction rules due to complex lattice

Table B.4 [p.29] summarizes the extinction rules due to complex lattice. In the following description, mathematical proofs for those due to base-centered, body-centered and face-centered lattice are given.

B.5.1.1 Extinction due to base-centered lattice

Symmetry of C base-centered lattice is described as follows,

$$\begin{aligned} \rho[T_C^{(i)}(\mathbf{r})] &= \rho[T_C^{(0)}(\mathbf{r})], \quad i \in \{0, 1\}. \\ T_C^{(0)}(\mathbf{r}) &= x\mathbf{a} + y\mathbf{b} + z\mathbf{c}, \\ T_C^{(1)}(\mathbf{r}) &= (x + \frac{1}{2})\mathbf{a} + (y + \frac{1}{2})\mathbf{b} + z\mathbf{c}. \end{aligned}$$

The extinction condition is described similarly to (B.2) as follows:

$$\sum_{i=0}^1 \exp[-i2\pi\mathbf{h} \cdot T_C^{(i)}(\mathbf{r})] = 0. \quad (\text{B.3})$$

Here, mathematical convenience to calculate \sum in (B.3), let us define $f_C(\mathbf{h}, \mathbf{r})$ as follows,

$$\begin{aligned} f_C(\mathbf{h}, \mathbf{r}) &= \exp\{-i2\pi[h(x + \frac{1}{4}) + k(y + \frac{1}{4}) + lz]\}. \end{aligned}$$

Therefore, the extinction condition is described as follows,

$$\begin{aligned} f_C(\mathbf{h}, \mathbf{r}) &\times \{\exp[-i\frac{\pi}{2}(h+k)] + \exp[+i\frac{\pi}{2}(h+k)]\} \\ &= 2f_C(\mathbf{h}, \mathbf{r}) \cos[\frac{\pi}{2}(h+k)] = 0. \end{aligned}$$

Since $f_C(\mathbf{h}, \mathbf{r})$ is not zero in general, the extinction condition is given by

$$\cos[\frac{\pi}{2}(h+k)] = 0.$$

Since the above equation is satisfied when $h+k$ is odd, the reflection condition (not extinct) as shown in Table B.4 [p.29] is given by

$$hkl : @h + k = 2n$$

Here, l is an arbitrary integer.

Reflection conditions for A and B base-centered lattice can be derived similarly to the above description.

B.5.1.2 Extinction due to body-centered lattice

Symmetry of body-centered lattice is described as follows,

$$\begin{aligned}\rho[T_I^{(i)}(\mathbf{r})] &= \rho[T_I^{(0)}(\mathbf{r})], \quad i \in \{0, 1\}. \\ T_I^{(0)}(\mathbf{r}) &= x\mathbf{a} + y\mathbf{b} + z\mathbf{c}, \\ T_I^{(1)}(\mathbf{r}) &= (x + \frac{1}{2})\mathbf{a} \\ &\quad + (y + \frac{1}{2})\mathbf{b} \\ &\quad + (z + \frac{1}{2})\mathbf{c}.\end{aligned}$$

The extinction condition is described similarly to (B.2) [p.33] as follows,

$$\sum_{i=0}^1 \exp[-i2\pi\mathbf{h} \cdot T_I^{(i)}(\mathbf{r})] = 0. \quad (\text{B.4})$$

For convenience for calculation of \sum in (B.4), let $f_I(\mathbf{h}, \mathbf{r})$ be defined as follows,

$$\begin{aligned}f_I(\mathbf{h}, \mathbf{r}) &= \exp\{-i2\pi[h(x + \frac{1}{4}) \\ &\quad + k(y + \frac{1}{4}) \\ &\quad + l(z + \frac{1}{4})]\}.\end{aligned}$$

Therefore, the extinction condition is given as follows,

$$\begin{aligned}f_I(\mathbf{h}, \mathbf{r}) \times \\ \{ \exp[-i\frac{\pi}{2}(h+k+l)] \\ + \exp[+i\frac{\pi}{2}(h+k+l)] \} \\ = 2f_I(\mathbf{h}, \mathbf{r}) \cos[\frac{\pi}{2}(h+k+l)] = 0.\end{aligned}$$

Since $f_I(\mathbf{h}, \mathbf{r})$ is not zero in general, the extinction condition is given by

$$\cos[\frac{\pi}{2}(h+k+l)] = 0.$$

Since the above equation is satisfied when $h+k+l$ is odd, the reflection condition (not extinct) as shown in Table B.4 [p.29], is given as follows,

$$hkl : \quad h+k+l = 2n$$

B.5.1.3 Extinction due to face-centered lattice

Symmetry of face-centered lattice is described as follows,

$$\begin{aligned}\rho[T_F^{(i)}(\mathbf{r})] &= \rho[T_F^{(0)}(\mathbf{r})], \quad i \in \{0, 1, 2, 3\}. \\ T_F^{(0)}(\mathbf{r}) &= x\mathbf{a} + y\mathbf{b} + z\mathbf{c}, \\ T_F^{(1)}(\mathbf{r}) &= x\mathbf{a} + (y + \frac{1}{2})\mathbf{b} + (z + \frac{1}{2})\mathbf{c}, \\ T_F^{(2)}(\mathbf{r}) &= (x + \frac{1}{2})\mathbf{a} + y\mathbf{b} + (z + \frac{1}{2})\mathbf{c}, \\ T_F^{(3)}(\mathbf{r}) &= (x + \frac{1}{2})\mathbf{a} + (y + \frac{1}{2})\mathbf{b} + z\mathbf{c}.\end{aligned}$$

The extinction condition is described similarly to (B.2) [p.33] by the following equation,

$$\sum_{i=0}^3 \exp[-i2\pi\mathbf{h} \cdot T_F^{(i)}(\mathbf{r})] = 0. \quad (\text{B.5})$$

Here, for mathematical convenience to calculate \sum in (B.5), let us define $f_F(\mathbf{h}, \mathbf{r})$ as follows,

$$\begin{aligned}f_F(\mathbf{h}, \mathbf{r}) &= \exp\{-i2\pi[h(x + \frac{1}{4}) \\ &\quad + k(y + \frac{1}{4}) \\ &\quad + l(z + \frac{1}{4})]\}.\end{aligned}$$

Therefore, the extinction condition is given as follows,

$$\begin{aligned}f_F(\mathbf{h}, \mathbf{r}) \{ \exp[-i\frac{\pi}{2}(-h-k-l)] \\ + \exp[-i\frac{\pi}{2}(-h+k+l)] \\ + \exp[-i\frac{\pi}{2}(+h-k+l)] \\ + \exp[-i\frac{\pi}{2}(+h+k-l)] \} \\ = 2f_F(\mathbf{h}, \mathbf{r}) \{ \exp(+i\frac{\pi}{2}h) \cos[\frac{\pi}{2}(k+l)] \\ + \exp(-i\frac{\pi}{2}h) \cos[\frac{\pi}{2}(k-l)] \} = 0.\end{aligned} \quad (\text{B.6})$$

$$\begin{aligned} = 2f_F(\mathbf{h}, \mathbf{r}) \{ \exp(+i\frac{\pi}{2}h) \cos[\frac{\pi}{2}(k+l)] \\ + \exp(-i\frac{\pi}{2}h) \cos[\frac{\pi}{2}(k-l)] \} = 0.\end{aligned} \quad (\text{B.7})$$

Since $f_F(\mathbf{h}, \mathbf{r})$ is not zero in general, the extinction condition is represented as follows,

$$\begin{aligned}\cos[\frac{\pi}{2}(k+l)] &= 0, \\ \cos[\frac{\pi}{2}(k-l)] &= 0.\end{aligned}$$

$[(k + l \text{ is even}) \text{ and } (k - l \text{ is even})]$ is identical to $[(\text{both } k \text{ and } l \text{ are even}) \text{ or } (\text{both } k \text{ and } l \text{ are odd})]$ i.e. $k + l = 2n$. Here, h is an arbitrary integer. Since (B.6) is symmetrical for h, k and l , equations similar to (B.7) can be derived also for $h + k, h - k$ and $h + l, h - l$. Then, The reflection condition (not distinguishing) as shown in Table B.4 [p.29] is given by

$$\begin{aligned}
 hkl : \quad h + k &= 2n, \\
 hkl : \quad h + l &= 2n, \\
 hkl : \quad l + k &= 2n.
 \end{aligned}$$

That is to say, reflection distinguishes when even and odd integers are mixed in h, k and l .

B.5.2 Extinction owing to glide axes

In cases of protein crystals, they do not have glide axis absolutely since they consist of only L amino acids but of not D amino acids (optical isomers of L amino acids).

B.5.2.1 Extinction due to axial glide plane

Symmetry due to c glide plane perpendicular to \mathbf{b} axis whose height is $\frac{1}{4}\mathbf{b}$, is given by

$$\begin{aligned}
 \rho[T_{Bc}^{(i)}(\mathbf{r})] &= \rho[T_{Bc}^{(0)}(\mathbf{r})], \quad i \in \{0, 1\}. \\
 T_{Bc}^{(0)}(\mathbf{r}) &= x\mathbf{a} + y\mathbf{b} + z\mathbf{c}, \\
 T_{Bc}^{(1)}(\mathbf{r}) &= x\mathbf{a} + \left(\frac{1}{2} - y\right)\mathbf{b} + \left(\frac{1}{2} + z\right)\mathbf{c},
 \end{aligned}$$

Similarly to (B.2) [p.33], the extinction condition is given by

$$\sum_{i=0}^1 \exp[-i2\pi\mathbf{h} \cdot T_{Bc}^{(i)}(\mathbf{r})] = 0. \quad (\text{B.8})$$

Here, for mathematical convenience to calculate \sum in (B.8) [p.35], let us define $f_{Bc}(\mathbf{h}, \mathbf{r})$ as follows,

$$\begin{aligned}
 f_{Bc}(\mathbf{h}, \mathbf{r}) &= \exp\left\{-i2\pi\left[hx + k\frac{1}{4} + l\left(\frac{1}{4} + z\right)\right]\right\}. \\
 f_{Bc}(\mathbf{h}, \mathbf{r}) \times \\
 &\left\{ \exp\left\{+i2\pi\left[k\left(\frac{1}{4} - y\right) + l\frac{1}{4}\right]\right\} \right. \\
 &+ \left. \exp\left\{-i2\pi\left[k\left(\frac{1}{4} - y\right) + l\frac{1}{4}\right]\right\} \right\} \\
 &= 2f_{Bc}(\mathbf{h}, \mathbf{r}) \cos\left\{\frac{\pi}{2}[k(1 - 4y) + l]\right\} = 0.
 \end{aligned}$$

Since $f_F(\mathbf{h}, \mathbf{r})$ is not zero in general, reflections distinguish when the term of $\cos\{\}$ is zero, i.e. when h is arbitrary, $k = 0$ and l is odd, the reflection condition as shown in Table B.5 [p.29] is given by

$$h0l : \quad l = 2n$$

B.5.2.2 Extinction due to double glide plane (e glide plane)

Therefore, Symmetry due to double glide plane (e glide plane) whose height is zero, is described as follows,

$$\begin{aligned}
 \rho[T_{Be}^{(i)}(\mathbf{r})] &= \rho[T_{Be}^{(0)}(\mathbf{r})], \quad i \in \{0, 1, 2, 3\}. \\
 T_{Be}^{(0)}(\mathbf{r}) &= x\mathbf{a} + y\mathbf{b} + z\mathbf{c}, \\
 T_{Be}^{(1)}(\mathbf{r}) &= \left(x + \frac{1}{2}\right)\mathbf{a} - y\mathbf{b} + z\mathbf{c}, \\
 T_{Be}^{(2)}(\mathbf{r}) &= x\mathbf{a} - y\mathbf{b} + \left(z + \frac{1}{2}\right)\mathbf{c}, \\
 T_{Be}^{(3)}(\mathbf{r}) &= \left(x + \frac{1}{2}\right)\mathbf{a} + y\mathbf{b} + \left(z + \frac{1}{2}\right)\mathbf{c},
 \end{aligned}$$

Similarly to (B.2) [p.33], the extinction rule is described by

$$\sum_{i=0}^3 \exp[-i2\pi\mathbf{h} \cdot T_{Be}^{(i)}(\mathbf{r})] = 0. \quad (\text{B.9})$$

Here, for mathematical convenience to calculate \sum in (B.9), let us define $f_{Be}(\mathbf{h}, \mathbf{r})$ as follows,

$$f_{Be}(\mathbf{h}, \mathbf{r}) = \exp\left\{-i2\pi\left[h\left(\frac{1}{4} + x\right) + l\left(\frac{1}{4} + z\right)\right]\right\}.$$

Therefore, the extinction condition can be described as follows,

$$\begin{aligned}
 &f_{Be}(\mathbf{h}, \mathbf{r}) \times \\
 &\left\{ \exp\left\{-i2\pi\left[-h\frac{1}{4} + ky - l\frac{1}{4}\right]\right\} \right. \\
 &+ \exp\left\{-i2\pi\left[+h\frac{1}{4} - ky - l\frac{1}{4}\right]\right\} \\
 &+ \exp\left\{-i2\pi\left[-h\frac{1}{4} - ky + l\frac{1}{4}\right]\right\} \\
 &+ \left. \exp\left\{-i2\pi\left[+h\frac{1}{4} + ky + l\frac{1}{4}\right]\right\} \right\} \\
 &= 2f_{Be}(\mathbf{h}, \mathbf{r}) \times \\
 &\left\{ \exp(-i2\pi ky) \cos\left[\frac{\pi}{2}(h + l)\right] \right. \\
 &+ \left. \exp(+i2\pi ky) \cos\left[\frac{\pi}{2}(h - l)\right] \right\} = 0.
 \end{aligned}$$

Since $f_{Be}(\mathbf{h}, \mathbf{r})$ and $\exp(\pm i2\pi ky)$ are not zero in general, the above extinction condition is satisfied when $\cos[\frac{\pi}{2}(h+l)] = 0 \cos[\frac{\pi}{2}(h-l)] = 0$. hkl reflections distinguishes when both $h+l$ and $h-l$ are odd, i.e. when k is arbitrary and $[(h, k \text{ are odd}) \text{ or } (h, k \text{ are even})]$. The reflection condition (not extinct) is given by

$$hkl : h + l = 2n$$

With regard to other double glide planes, extinction rules as shown in Table B.5 [p.29] can be derived in a similar way.

B.5.2.3 Extinction due to diagonal glide plane

Symmetry due to diagonal glide plane (n glide plane) whose height is zero, is described as follows,

$$\rho[T_{Bn}^{(i)}(\mathbf{r})] = \rho[T_{Bn}^{(0)}(\mathbf{r})], \quad i \in \{0, 1\}.$$

$$T_{Bn}^{(0)}(\mathbf{r}) = x\mathbf{a} + y\mathbf{b} + z\mathbf{c},$$

$$T_{Bn}^{(1)}(\mathbf{r}) = (\frac{1}{2} + x)\mathbf{a} - y\mathbf{b} + (\frac{1}{2} + z)\mathbf{c},$$

The extinction condition is described similarly to (B.2) [p.33] as follows,

$$\sum_{i=0}^1 \exp[-i2\pi \mathbf{h} \cdot T_{Bn}^{(i)}(\mathbf{r})] = 0. \quad (\text{B.10})$$

Here, mathematical convenience to calculate \sum in (B.10), let us define $f_{Bn}(\mathbf{h}, \mathbf{r})$ as follows,

$$f_{Bn}(\mathbf{h}, \mathbf{r}) = \exp\{-i2\pi[h(\frac{1}{4} + x) + l(\frac{1}{4} + z)]\}.$$

Therefore, the extinction condition is described as follows,

$$\begin{aligned} & f_{Bn}(\mathbf{h}, \mathbf{r}) \times \\ & \left\{ \exp\{-i2\pi[-h\frac{1}{4} + ky - l\frac{1}{4}]\} \right. \\ & \left. + \exp\{-i2\pi[h\frac{1}{4} - ky + l\frac{1}{4}]\} \right\} \\ & = 2f_{Bn}(\mathbf{h}, \mathbf{r}) \cos\{\frac{\pi}{2}[4ky - (h+l)]\} = 0. \end{aligned}$$

Since $f_{Bn}(\mathbf{h}, \mathbf{r})$ is not zero in general, hkl reflections distinguish when the term of $\cos\{\}$ is zero. Therefore, the reflection condition (not extinct) is described as follows,

$$h0l : h + l = 2n$$

With regard to other orthogonal glide plane, reflection conditions as summarized in Table B.5 [p.29] can be derived.

B.5.3 Extinction due to screw axes

Table B.6 [p.30] summarizes extinction rules due to p_q screw axes. Here $p \in \{2, 3, 4, 6\}$ and $q \in \{1, \dots, p-1\}$, p_q screw axis makes p equivalent points such that they translate by $q\mathbf{c}/p$, ($q\mathbf{a}/p$ or $q\mathbf{b}/p$) when rotated by $2\pi/p$ around the axis. As summarized in Table B.6 [p.30], reflection condition $[00l : l = 2n]$ is given by 2_1 , 4_2 and 6_3 screw axes since they make layers of atoms (molecules) whose spacing is c , (a or b).

Similarly, reflection conditions $[000l : l = 3n]$ for 3_1 , 3_2 , 6_2 , 6_4 screw axes, $[00l : l = 4n]$ for 4_1 , 4_3 screw axes and $[000l : l = 6n]$ for 6_1 , 6_5 screw axes can be derived. For mathematical proof of reflection conditions for three- and six-fold screw axes, refer to Appendix C [p.39], please.

In the following description, mathematical proofs of extinction rules due to 2_1 , 4_1 and 4_2 screw axes.

B.5.3.1 Extinction due to 2_1 screw axis

Symmetry of 2_1 screw axis in the direction of \mathbf{c} located at $\frac{1}{2}\mathbf{a} + \frac{1}{2}\mathbf{b}$, is described as follows,

$$\rho[T_{2_1}^{(i)}(\mathbf{r})] = \rho[T_{2_1}^{(0)}(\mathbf{r})], \quad i \in \{0, 1\}.$$

$$T_{2_1}^{(0)}(\mathbf{r}) = (\frac{1}{2} + x)\mathbf{a} + (\frac{1}{2} + y)\mathbf{b} + z\mathbf{c},$$

$$T_{2_1}^{(1)}(\mathbf{r}) = (\frac{1}{2} - x)\mathbf{a} + (\frac{1}{2} - y)\mathbf{b} + (\frac{1}{2} + z)\mathbf{c}.$$

The extinction condition is described similarly to (B.2) [p.33] as follows,

$$\sum_{i=0}^1 \exp[-i2\pi \mathbf{h} \cdot T_{2_1}^{(i)}(\mathbf{r})] = 0. \quad (\text{B.11})$$

Here, for mathematical convenience to calculate \sum of (B.11), let us define $f_{2_1}(\mathbf{h}, \mathbf{r})$ as follows,

$$f_{2_1}(\mathbf{h}, \mathbf{r}) = \exp\{-i2\pi[h\frac{1}{2} + k\frac{1}{2} + l(\frac{1}{4} + z)]\}.$$

Therefore, summation in (B.11) can be deformed to give the following extinction condi-

tion,

$$\begin{aligned}
 & f_{2_1}(\mathbf{h}, \mathbf{r}) \times \\
 & \left\{ \exp\{-i2\pi[hx + ky - l\frac{1}{4}]\} \right. \\
 & \left. + \exp\{-i2\pi[-hx - ky + l\frac{1}{4}]\} \right\} \\
 & = f_{2_1}(\mathbf{h}, \mathbf{r}) \times \\
 & \cos\left\{\frac{\pi}{2}[4(hx + ky) - l]\right\} = 0.
 \end{aligned}$$

Since term of $\cos\{ \}$ is zero when $h, k = 0$ and l is odd, the reflection condition (not extinct) is given by

$$00l : \quad l = 2n.$$

Similarly, the reflection conditions due to \mathbf{c} and \mathbf{a} screw axes can be obtained as summarized in Table B.6 [p.30].

B.5.3.2 Extinction due to 4_1 screw axis

Symmetry due to 4_1 screw axis that is located at the origin, can be described as follows,

$$\begin{aligned}
 \rho[T_{4_1}^{(i)}(\mathbf{r})] &= \rho[T_{4_1}^{(0)}(\mathbf{r})], \quad i \in \{0, 1, 2, 3\}. \\
 T_{4_1}^{(0)}(\mathbf{r}) &= +x\mathbf{a} + y\mathbf{b} + \frac{1}{8}\mathbf{c}, \\
 T_{4_1}^{(1)}(\mathbf{r}) &= -y\mathbf{a} + x\mathbf{b} + \frac{3}{8}\mathbf{c}, \\
 T_{4_1}^{(2)}(\mathbf{r}) &= -x\mathbf{a} - y\mathbf{b} + \frac{5}{8}\mathbf{c}, \\
 T_{4_1}^{(3)}(\mathbf{r}) &= +y\mathbf{a} - x\mathbf{b} + \frac{7}{8}\mathbf{c}.
 \end{aligned}$$

Here, the extinction condition is described similarly to (B.2) [p.33] as follows,

$$\sum_{i=0}^3 \exp[-i2\pi\mathbf{h} \cdot T_{4_1}^{(i)}(\mathbf{r})] = 0. \quad (\text{B.12})$$

Here, let us define $f_{4_1}(\mathbf{h}, \mathbf{r})$ as follows,

$$f_{4_1}(\mathbf{h}, \mathbf{r}) = \exp(-i2\pi l \frac{1}{2}).$$

Therefore, summation in (B.12) can be deformed to give the following extinction condi-

tion,

$$\begin{aligned}
 & f_{4_1}(\mathbf{h}, \mathbf{r}) \times \\
 & \left\{ \exp[-i2\pi(+hx + ky - l\frac{3}{8})] \right. \\
 & + \exp[-i2\pi(-hy + kx - l\frac{1}{8})] \\
 & + \exp[-i2\pi(-hx - ky + l\frac{1}{8})] \\
 & \left. + \exp[-i2\pi(+hy - kx + l\frac{3}{8})] \right\} \\
 & = 2f_{4_1}(\mathbf{h}, \mathbf{r}) \times \\
 & \left\{ \exp(+i2\pi l \frac{1}{8}) \cos\left\{\frac{\pi}{2}[4(hx + ky) - l]\right\} \right. \\
 & \left. + \exp(-i2\pi l \frac{1}{8}) \cos\left\{\frac{\pi}{2}[4(hy - kx) + l]\right\} \right\} \\
 & = 0.
 \end{aligned}$$

When $h, k = 0$ and l is even, $\cos\{ \}$ in the first and second terms of the above equation have an identical value (1 or -1). Under an assumption that this condition is satisfied, let us discuss the condition that the above equation gives value of zero as follows,

$$\begin{aligned}
 & \exp(-i2\pi l \frac{1}{8}) + \exp(-i2\pi l \frac{1}{8}) \\
 & = 2 \cos\left(\frac{\pi}{2} \cdot \frac{l}{2}\right) = 0.
 \end{aligned}$$

The above equation means that reflections distinguish when $l/2$ is odd. Therefore, the reflection condition (not extinct) can be described as follows,

$$00l : \quad l = 4n.$$

Similarly, reflection condition due to 4_3 screw axis can be obtained.

B.5.3.3 Extinction due to 4_2 screw axis

Symmetry due to 4_2 screw axis at the origin can be describes as follows,

$$\begin{aligned}
 \rho[T_{4_2}^{(i)}(\mathbf{r})] &= \rho[T_{4_2}^{(0)}(\mathbf{r})], \quad i \in \{0, 1, 2, 3\}. \\
 T_{4_2}^{(0)}(\mathbf{r}) &= +x\mathbf{a} + y\mathbf{b} + \frac{1}{4}\mathbf{c}, \\
 T_{4_2}^{(1)}(\mathbf{r}) &= -y\mathbf{a} + x\mathbf{b} + \frac{3}{4}\mathbf{c}, \\
 T_{4_2}^{(2)}(\mathbf{r}) &= -x\mathbf{a} - y\mathbf{b} + \frac{1}{4}\mathbf{c}, \\
 T_{4_2}^{(3)}(\mathbf{r}) &= +y\mathbf{a} - x\mathbf{b} + \frac{3}{4}\mathbf{c}.
 \end{aligned}$$

A point translates by $\frac{2}{4}\mathbf{c}$ when rotating by $\frac{2\pi}{4}$ around the axis. Here, note that the heights of $T_{4_2}^{(2)}(\mathbf{r})$ and $T_{4_2}^{(3)}(\mathbf{r})$ are $\frac{5}{4}\mathbf{c}$ and $\frac{7}{4}\mathbf{c}$ which are equivalent to $\frac{1}{4}\mathbf{c}$, $\frac{3}{4}\mathbf{c}$ due to translation symmetry of unit cell.

The, the extinction condition is described similarly to (B.2) [p.33] as follows,

$$\sum_{i=0}^3 \exp[-i2\pi\mathbf{h} \cdot T_{4_2}^{(i)}] = 0. \quad (\text{B.13})$$

Here, for mathematical convenience to calculate \sum in (B.13), let $f_{4_2}(\mathbf{h}, \mathbf{r})$ be dined as follows,

$$f_{4_2}(\mathbf{h}, \mathbf{r}) = \exp[-i2\pi(l\frac{1}{2})].$$

$f_{4_2}(\mathbf{h}, \mathbf{r})$ Therefore, deforming the \sum of (B.13), the extinction condition can be obtained as follows,

$$\begin{aligned} & f_{4_2}(\mathbf{h}, \mathbf{r}) \times \\ & \left\{ \exp[-i2\pi(+hx + ky - l\frac{1}{4})] \right. \\ & + \exp[-i2\pi(-ky + hx + l\frac{1}{4})] \\ & + \exp[-i2\pi(-hx - ky - l\frac{1}{4})] \\ & \left. + \exp[-i2\pi(+kx - hy + l\frac{1}{4})] \right\} \end{aligned}$$

$$\begin{aligned} & = 2f_{4_2}(\mathbf{h}, \mathbf{r}) \times \\ & \left\{ \exp(+i2\pi l\frac{1}{4}) \cos[2\pi(hx + ky)] \right. \\ & \left. + \exp(-i2\pi l\frac{1}{4}) \cos[2\pi(kx - hy)] \right\} \\ & = 0. \end{aligned}$$

The above extinction can be discussed when the content of $\cos[]$ is zero. Under the assumption that the above condition is satisfied, the above equation can be further deformed as follows,

$$\begin{aligned} & \exp(-i2\pi l\frac{1}{4}) + \exp(+i2\pi l\frac{1}{4}) \\ & = 2 \cos(\frac{\pi}{2}l) = 0. \end{aligned}$$

Therefore, the reflection condition (not extinct) can be described as follows,

$$00l : l = 2n.$$

Reflection condition due to 6_3 screw axis is the same as the above description. With regard to this, refer to §C.2.5 [p.44] in Appendix C, please.

Appendix C

Reflection indices and extinction rules in the cases of trigonal and hexagonal crystals

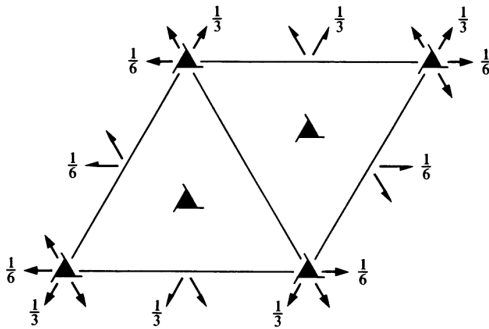


Figure C.1: *International Tables for Crystallography* (2006) Vol.A, Symmetric elements. $P3_121$ (#152).

Read this chapter when the reader has time, please.

In cases of trigonal and hexagonal crystal system, reflection vectors are usually indexed by four integers, $h k i l$ ($h + k + i = 0$). This chapter describes the reasonableness of this way of indexing and the extinction rules due to three- and six-fold screw axes.

C.1 Cases of trigonal system

C.1.1 Diagram shown in *International Tables for Crystallography* (2006) Vol.A

Fig. C.1 is a diagram in *International Tables for Crystallography* (2006) Vol.A that

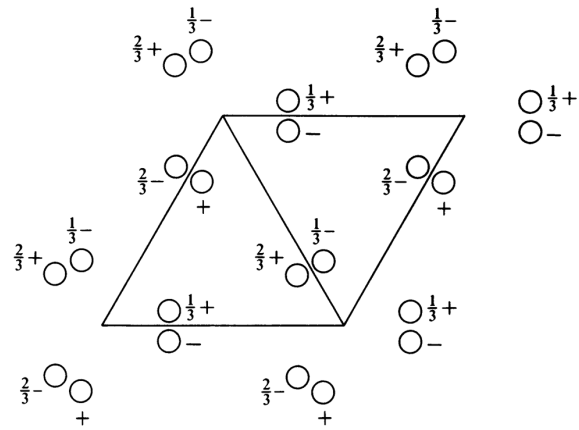


Figure C.2: *International Tables for Crystallography* (2006) Vol.A, Positions of atoms. $P3_121$ (#152).

shows symmetric elements of space group $P3_121$ (#152). Fig. C.2 shows atomic coordinates of $P3_121$ (#152).

The unit cell is usually taken to be a rhombus that consists of two regular triangles as shown in Figs. C.1 and C.2. Space group $P3_121$ (#152) has three-fold screw axis in the direction of \mathbf{c} axis and two-fold screw axis perpendicular to \mathbf{c} axis. However, in the case of trigonal system, there is no extinction due to the two-fold screw axis. About this, refer to the description in §C.1.4 [p.41], please.

C.1.2 Real and reciprocal coordinates

Fig. C.3 shows real and reciprocal primitive translation vectors in the cases of trigonal and hexagonal crystal system.

\mathbf{a} , \mathbf{b} and \mathbf{c} axes are usually taken such that the angle spanned by \mathbf{a} and \mathbf{b} axes is 120° and \mathbf{c} is parallel to three-fold rotation or screw axis. There are three way of taking \mathbf{a} and \mathbf{b} axes as shown in Fig. C.3 i.e. combinations of \mathbf{a}_0 and \mathbf{b}_0 axes, \mathbf{a}_1 and \mathbf{b}_1 axes and \mathbf{a}_2 and \mathbf{b}_2 axes.

reciprocal primitive vectors are defined as follows:

$$\begin{aligned}\mathbf{a}^* &= \frac{\mathbf{b} \times \mathbf{c}}{\mathbf{a} \cdot (\mathbf{b} \times \mathbf{c})}, \\ \mathbf{b}^* &= \frac{\mathbf{c} \times \mathbf{a}}{\mathbf{a} \cdot (\mathbf{b} \times \mathbf{c})}, \\ \mathbf{c}^* &= \frac{\mathbf{a} \times \mathbf{b}}{\mathbf{a} \cdot (\mathbf{b} \times \mathbf{c})}.\end{aligned}$$

About the reasonableness of the above definition, refer to Appendix A [p.22], please.

By following the above definition, in Fig. C.3, real (black) and reciprocal (gray) primitive translation vectors are drawn. Referring to this figure, the following relations can easily be understood,

$$\begin{aligned}\mathbf{a}_0^* &= -\mathbf{b}_1^* \\ &= -\mathbf{a}_2^* + \mathbf{b}_2^*, \\ \mathbf{b}_0^* &= \mathbf{a}_1^* - \mathbf{b}_1^* \\ &= -\mathbf{a}_2^*.\end{aligned}$$

From the above relations, reciprocal lattice vector $h\mathbf{a}_0^* + k\mathbf{b}_0^* + l\mathbf{c}^*$ can also be represented as follows:

$$\begin{aligned}h\mathbf{a}_0^* + k\mathbf{b}_0^* + l\mathbf{c}^* &= k\mathbf{a}_1^* + i\mathbf{b}_1^* + l\mathbf{c}^* \\ &= i\mathbf{a}_2^* + h\mathbf{b}_2^* + l\mathbf{c}^*,\end{aligned}$$

where, $h + k + i = 0$.

By using four indices h , k , i and l ($h+k+i=0$) to describe reflections, we can easily understand the equivalence of reflections due to three-fold symmetry. For example, a reflection described as $1\ 1\ 0$ by using $\mathbf{a}_0^*\text{-}\mathbf{b}_0^*\text{-}\mathbf{c}^*$ coordinate system is equivalent to $1\ \bar{2}\ 0$ by $\mathbf{a}_1^*\text{-}\mathbf{b}_1^*\text{-}\mathbf{c}^*$ system and also to $\bar{2}\ 1\ 0$ by $\mathbf{a}_2^*\text{-}\mathbf{b}_2^*\text{-}\mathbf{c}^*$ system. This reflection $1\ 1\ \bar{2}\ 0$ described using four indices can easily be understood to be equivalent to $1\ \bar{2}\ 1\ 0$ and $\bar{2}\ 1\ 1\ 0$.

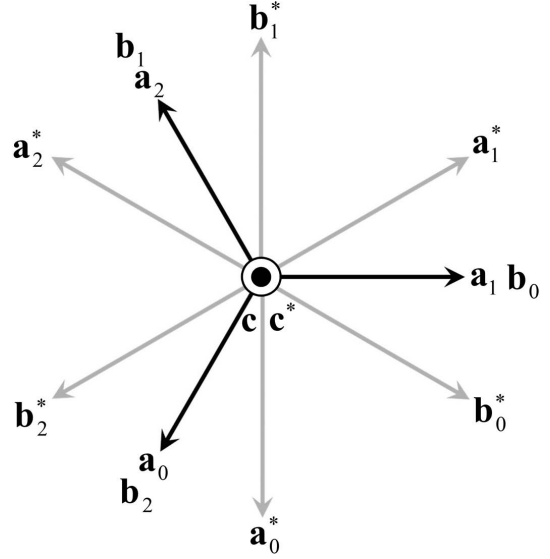


Figure C.3: Real (black) and reciprocal (gray) primitive translation vectors.

C.1.3 Derivation of extinction rule due to 3_1 screw axis

Similarly to the description in Appendix B §B.5 [p.33], the extinction due to 3_1 screw axis can be derived as follows.

Symmetry due to 3_1 screw axis at the origin is described as follows:

$$\begin{aligned}\rho[T_{3_1}^{(i)}(\mathbf{r})] &= \rho[T_{3_1}^{(0)}(\mathbf{r})], \quad i \in \{0, 1, 2\}. \\ T_{3_1}^{(0)}(\mathbf{r}) &= x\mathbf{a}_0 + y\mathbf{b}_0 + z\mathbf{c}, \\ T_{3_1}^{(1)}(\mathbf{r}) &= x\mathbf{a}_1 + y\mathbf{b}_1 + \left(\frac{1}{3} + z\right)\mathbf{c}, \\ T_{3_1}^{(2)}(\mathbf{r}) &= x\mathbf{a}_2 + y\mathbf{b}_2 + \left(\frac{2}{3} + z\right)\mathbf{c}.\end{aligned}\quad (\text{C.1})$$

On the other hand, referring to Fig. C.3, the following relations are evident.

$$\begin{aligned}\mathbf{a}_1 &= \mathbf{b}_0, \\ \mathbf{b}_1 &= -\mathbf{a}_0 - \mathbf{b}_0, \\ \mathbf{a}_2 &= -\mathbf{a}_0 - \mathbf{b}_0, \\ \mathbf{b}_2 &= \mathbf{a}_0,\end{aligned}$$

Substituting the above equation into (C.1),

$$\begin{aligned}\rho[T_{3_1}^{(i)}(\mathbf{r})] &= \rho[T_{3_1}^{(0)}(\mathbf{r})], \quad i \in \{0, 1, 2\}. \\ T_{3_1}^{(0)}(\mathbf{r}) &= x\mathbf{a}_0 + y\mathbf{b}_0 + z\mathbf{c}, \\ T_{3_1}^{(1)}(\mathbf{r}) &= -y\mathbf{a}_0 + (x - y)\mathbf{b}_0 + \left(\frac{1}{3} + z\right)\mathbf{c}, \\ T_{3_1}^{(2)}(\mathbf{r}) &= (-x + y)\mathbf{a}_0 - x\mathbf{b}_0 + \left(\frac{2}{3} + z\right)\mathbf{c}.\end{aligned}$$

The extinction condition can be described similarly to (B.2) [p.33] as follows:

$$\sum_{i=0}^2 \exp[-i2\pi \mathbf{h} \cdot T_{3_1}^{(i)}(\mathbf{r})] = 0. \quad (\text{C.2})$$

Here, for mathematical convenience to calculate \sum of (C.2), let us define $f_{3_1}(\mathbf{h}, \mathbf{r})$ as follows:

$$f_{3_1}(\mathbf{h}, \mathbf{r}) = \exp[-i2\pi(lz)].$$

Therefore, (C.2) can be deformed as follows:

$$\begin{aligned} & f_{3_1}(\mathbf{h}, \mathbf{r}) \times \\ & \left\{ \exp\{-i2\pi[hx + ky]\} \right. \\ & + \exp\{-i2\pi[-hy + k(x - y) + l\frac{1}{3}]\} \\ & \left. + \exp\{-i2\pi[+h(-x + y) - kx + l\frac{2}{3}]\} \right\} = 0. \end{aligned}$$

Since terms $[hx + ky]$, $[-hy + k(x - y)]$ and $[h(-x + y) - kx]$ in $\exp\{ \}$ of the above equation depend on value of x and y , the extinction can be discussed only when $h = k = l = 0$. Under this condition, the extinction condition can be described as follows:

$$1 + \exp(-i2\pi l \frac{1}{3}) + \exp(-i2\pi l \frac{2}{3}) = 0.$$

The second and third terms of on the left-hand side of the above equation are 1 and 1 not giving extinction when $l = 3n$, $\exp(-i2\pi \frac{1}{3})$ and $\exp(-i2\pi \frac{2}{3})$ giving extinction and $\exp(-i2\pi \frac{2}{3})$ and $\exp(-i2\pi \frac{1}{3})$ giving extinction. Therefore, the reflection condition can be described as follows:

$$000l : l = 3n.$$

With similar consideration, the same reflection condition for 3_2 can be derived.

C.1.4 On the absence of extinction due to 2_1 screw axis perpendicular to \mathbf{c} .

In Fig. C.1 [p.39], there are 2_1 screw axes perpendicular to \mathbf{c} at positions of $x = \frac{1}{2}$ and $y = \frac{1}{2}$. However, these 2_1 screw axes cause no extinction. The reason is that the angle spanned by \mathbf{a} and \mathbf{a}^* and that spanned by \mathbf{b} and \mathbf{b}^* are not zero (not parallel). About this, refer to the following description, please.

Symmetric operation due to rotation around \mathbf{a}_0 is represented by movement of point on a plane perpendicular to \mathbf{a}_0 . Referring to Fig. C.3, reciprocal vectors perpendicular to \mathbf{a}_0 are \mathbf{c}_0^* and \mathbf{b}_0^* . A real vector parallel to \mathbf{b}_0^* is represented by a linear combination of \mathbf{a}_0 and \mathbf{b}_0 , as $\frac{1}{2}\mathbf{a}_0 + \mathbf{b}_0$. Therefore, Symmetry due to 2_1 screw axis in the direction of \mathbf{a}_0 located at $(y, z) = \frac{1}{2}, \frac{1}{3}$ is represented as follows:

$$\begin{aligned} \rho[T_{2_1}^{(i)}(\mathbf{r})] &= \rho[T_{2_1}^{(0)}(\mathbf{r})], \quad i \in \{0, 1\}. \\ T_{2_1}^{(0)}(\mathbf{r}) &= x\mathbf{a}_0 \\ &+ (\frac{1}{2} + y)(\frac{1}{2}\mathbf{a}_0 + \mathbf{b}_0) \\ &+ (\frac{1}{3} + z)\mathbf{c} \\ &= (x + \frac{1}{4} + \frac{1}{2}y)\mathbf{a}_0 \\ &+ (\frac{1}{2} + y)\mathbf{b}_0 \\ &+ (\frac{1}{3} + z)\mathbf{c}, \\ T_{2_1}^{(1)}(\mathbf{r}) &= (\frac{1}{2} + x)\mathbf{a}_0 \\ &+ (\frac{1}{2} - y)(\frac{1}{2}\mathbf{a}_0 + \mathbf{b}_0) \\ &+ (\frac{1}{3} - z)\mathbf{c} \\ &= (x + \frac{3}{4} - \frac{1}{2}y)\mathbf{a}_0 \\ &+ (\frac{1}{2} - y)\mathbf{b}_0 \\ &+ (\frac{1}{3} - z)\mathbf{c}. \end{aligned}$$

The extinction condition (while not existing) is represented similarly to (B.2) [p.33] as follows:

$$\sum_{i=0}^1 \exp[-i2\pi \mathbf{h} \cdot T_{2_1}^{(i)}(\mathbf{r})] = 0. \quad (\text{C.3})$$

Here, for mathematical convenience to calculate \sum of (C.3), let us define $f_{2_1}(\mathbf{h}, \mathbf{r})$ as follows:

$$f_{2_1}(\mathbf{h}, \mathbf{r}) = \exp\{-i2\pi[h(\frac{1}{2} + x) + k\frac{1}{2} + l\frac{1}{3}]\}.$$

Therefore, \sum of (C.3) can be deformed as fol-

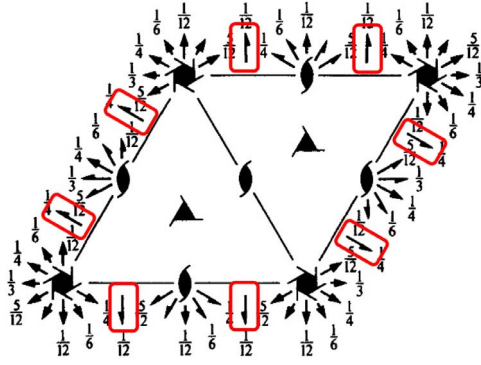


Figure C.4: *International Tables for Crystallography* (2006) Vol.A, Symmetric elements. $P6_122$ (#178).

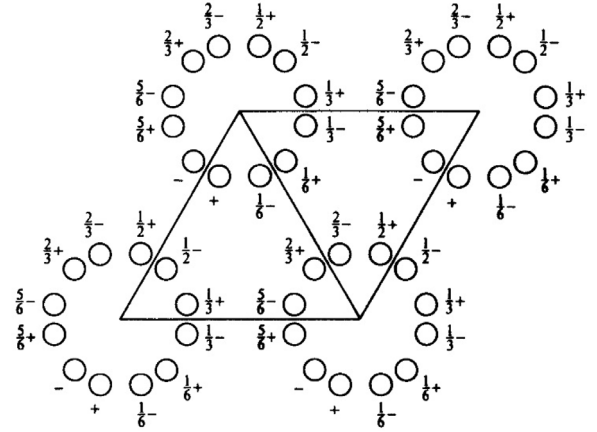


Figure C.5: *International Tables for Crystallography* (2006) Vol.A, Positions of atoms. $P6_122$ (#178).

lows:

$$\begin{aligned}
 & f_{2_1}(\mathbf{h}, \mathbf{r}) \times \\
 & \left\{ \exp\left\{-i2\pi\left[h\left(\frac{1}{4} - \frac{1}{2}y\right) - ky - lz\right]\right\} \right. \\
 & \left. + \exp\left\{-i2\pi\left[-h\left(\frac{1}{4} - \frac{1}{2}y\right) + ky + lz\right]\right\} \right\} \\
 & = f_{2_1}(\mathbf{h}, \mathbf{r}) \times \\
 & \cos\left\{2\pi\left[h\left(\frac{1}{4} - \frac{1}{2}y\right) - ky - lz\right]\right\} = 0.
 \end{aligned}$$

The above equation reveals that there is no extinction due to 2_1 screw axis perpendicular to \mathbf{c} since terms of h , k and l all depend to values of y or z . The second term $-h\frac{1}{2}y$ in $\cos\{ \}$ of the above equation exists since \mathbf{a}_0 is not parallel to \mathbf{a}_0^* . If there were a reciprocal primitive vector parallel to the screw axis, we can discuss the extinction under the condition that $k, l = 0$. When there is no reciprocal primitive vector parallel to the screw axis, there is no extinction due to it.

In a similar way, it can be verified that there is no extinction due to screw axes parallel to \mathbf{b}_0 or $\mathbf{a}_0 + \mathbf{b}_0$.

C.2 Case of hexagonal system

C.2.1 Figure shown in *International Tables for Crystallography* (2006) Vol.A

Fig. C.4 is a drawing for space group $P6_122$ (#178) in *International Tables for Crystallography* (2006) Vol.A that shows symmetric elements. Fig. C.5 shows coordinates of atoms.

The unit cell is usually taken similarly to that in the case of trigonal system as shown in Fig. C.1 [p.39] and C.2 [p.39]. There are 2_1 screw axes perpendicular to \mathbf{c} . However they do not cause extinction similarly to the case of trigonal system.

C.2.2 Coordinates for describing six-fold screw axes

For describing positions of atoms that are rotated by $\frac{i}{6}2\pi$ ($i \in \{0, 1, 2, 3, 4, 5\}$) from the original position, let us prepare combinations of \mathbf{a}_i and \mathbf{b}_i as follows:

\mathbf{a}_i	\mathbf{b}_i	i
\mathbf{a}_0	\mathbf{b}_0	0
$\mathbf{a}_0 + \mathbf{b}_0$	$-\mathbf{a}_0$	1
\mathbf{b}_0	$-\mathbf{a}_0 - \mathbf{b}_0$	2
$-\mathbf{a}_0$	$-\mathbf{b}_0$	3
$-\mathbf{a}_0 - \mathbf{b}_0$	\mathbf{a}_0	4
$-\mathbf{b}_0$	$\mathbf{a}_0 + \mathbf{b}_0$	5

By using the above coordinates, positions that is rotated by $\frac{i}{6}2\pi$ ($i \in \{0, 1, 2, 3, 4, 5\}$) from the

original position can be written as follows:

$$\begin{aligned} x_0 &= x, & y_0 &= y, \\ x_1 &= x - y, & y_1 &= x, \\ x_2 &= -y, & y_2 &= x - y, \\ x_3 &= -x, & y_3 &= -y, \\ x_4 &= -x + y, & y_4 &= -x, \\ x_5 &= y, & y_5 &= -x + y. \end{aligned}$$

C.2.3 Derivation of extinction rule due to 6_1 screw axis

Symmetry due to 6_1 screw axis located at the origin in the direction of \mathbf{c} , is described as follows:

$$\begin{aligned} \rho[T_{6_1}^{(i)}(\mathbf{r})] &= \rho[T_{6_1}^{(0)}(\mathbf{r})], \quad i \in \{0, 1, 2, 3, 4, 5\}. \\ T_{6_1}^{(0)}(\mathbf{r}) &= x\mathbf{a}_0 + y\mathbf{b}_0 + z\mathbf{c}, \\ T_{6_1}^{(1)}(\mathbf{r}) &= (x - y)\mathbf{a}_0 + x\mathbf{b}_0 + \left(\frac{1}{6} + z\right)\mathbf{c}, \\ T_{6_1}^{(2)}(\mathbf{r}) &= -y\mathbf{a}_0 + (x - y)\mathbf{b}_0 + \left(\frac{2}{6} + z\right)\mathbf{c}, \\ T_{6_1}^{(3)}(\mathbf{r}) &= -x\mathbf{a}_0 - y\mathbf{b}_0 + \left(\frac{3}{6} + z\right)\mathbf{c}, \\ T_{6_1}^{(4)}(\mathbf{r}) &= (-x + y)\mathbf{a}_0 - x\mathbf{b}_0 + \left(\frac{4}{6} + z\right)\mathbf{c}, \\ T_{6_1}^{(5)}(\mathbf{r}) &= y\mathbf{a}_0 + (-x + y)\mathbf{b}_0 + \left(\frac{5}{6} + z\right)\mathbf{c}. \end{aligned}$$

Similarly to (B.2) [p.33], the extinction condition is described as follows:

$$\sum_{i=0}^5 \exp[-i2\pi\mathbf{h} \cdot T_{6_1}^{(i)}(\mathbf{r})] = 0. \quad (\text{C.4})$$

For mathematical convenience, let us define $f_{6_1}(\mathbf{h}, \mathbf{r})$ as follows:

$$f_{6_1}(\mathbf{h}, \mathbf{r}) = \exp[-i2\pi(lz)].$$

From (C.4), the extinction condition is obtained as follows:

$$\begin{aligned} f_{6_1}(\mathbf{h}, \mathbf{r}) \times \\ \left\{ \exp\{-i2\pi[hx + ky]\} \right. \\ + \exp\{-i2\pi[h(x - y) + kx + l\frac{1}{6}]\} \\ + \exp\{-i2\pi[-hy + k(x - y) + l\frac{2}{6}]\} \\ + \exp\{-i2\pi[-hx - ky + l\frac{3}{6}]\} \\ + \exp\{-i2\pi[h(-x + y) - kx + l\frac{4}{6}]\} \\ \left. + \exp\{-i2\pi[hy + k(-x + y) + l\frac{5}{6}]\} \right\} = 0. \end{aligned}$$

The extinction can be discussed only when $h = k = i = 0$. Under this condition, the above extinction condition can be described as follows:

$$\begin{aligned} 1 \\ + \exp(-i2\pi l \frac{1}{6}) \\ + \exp(-i2\pi l \frac{2}{6}) \\ + \exp(-i2\pi l \frac{3}{6}) \\ + \exp(-i2\pi l \frac{4}{6}) \\ + \exp(-i2\pi l \frac{5}{6}) = 0. \quad (\text{C.5}) \end{aligned}$$

When $l = 6n$, reflections do not distinguish. When $l = 6n + i$ ($i \in \{1, 2, 3, 4, 5\}$), reflections distinguish since phase interval of the six term is an identical value $-2\pi\frac{i}{6}$. The reflection condition (not extinct) can be described as follows,

$$hkil : l = 6n.$$

Similarly, the same reflection condition can be derived also for 6_1 screw axis.

In Fig. C.4, 2_1 and 3_1 screw axes in the direction of \mathbf{c} are found. However, the logical product of reflection conditions due to 6_1 , 2_1 and 3_1 screw axes gives the same reflection condition as described in the above equation.

C.2.4 Derivation of the extinction due to 6_2 screw axis

The extinction condition due to 6_2 screw axis is given similarly to (C.5) [p.43] as follows:

$$\begin{aligned}
 &1 \\
 &+ \exp(-i2\pi l \frac{1}{3}) \\
 &+ \exp(-i2\pi l \frac{2}{3}) \\
 &+ 1 \\
 &+ \exp(-i2\pi l \frac{1}{3}) \\
 &+ \exp(-i2\pi l \frac{2}{3}) = 0.
 \end{aligned}$$

When $l = 3n$, reflections do not distinguish since the six terms have an identical value unity. When $l = 3n + i$ ($i \in \{1, 2\}$), reflections distinguish since phase interval of the six terms is an identical value $-2\pi \frac{i}{3}$. Then, the reflection condition (not extinct) is given by

$$hkl : l = 3n.$$

In a similar way, the same reflection condition

can be derived for 6_4 screw axis.

C.2.5 Derivation of extinction rule due to 6_3 screw axis

An equation for 6_3 screw axis that corresponds to (C.5) [p.43] is given by

$$\begin{aligned}
 &1 \\
 &+ \exp(-i2\pi l \frac{1}{2}) \\
 &+ 1 \\
 &+ \exp(-i2\pi l \frac{1}{2}) \\
 &+ 1 \\
 &+ \exp(-i2\pi l \frac{1}{2}) = 0.
 \end{aligned}$$

When l is even, all terms are unity giving no extinction. When l is odd, reflections distinguish since phase interval of the six terms is an identical value $-2\pi \frac{1}{2}$ giving extinction. Therefore, the reflection condition (not extinct) is given by

$$hkl : l = 2n.$$

End of the document.

Appendix D

Obtaining 3D data of the crystal shape

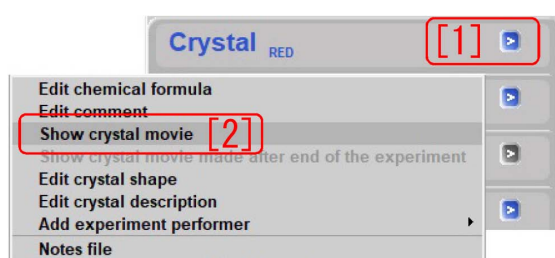


Figure D.1: Menu of ‘Crystal tab’

D.1 Abstract

The sequence of obtaining 3D data of the crystal outline is as follows:

1. By clicking [1] and then [2] in Fig. D.1, let Fig. D.2 be shown,
2. With ‘Point’ checked in [4] of Fig. D.2, click [1],[2],[3],[4] and finally [1] again. After turning the crystal image by 90° by clicking Fig. D.4 [7] Turn 90’, make a ‘box’ including the crystal as shown in Fig. D.6 [p.47] also by clicking [1],[2],[3],[4] and finally [1] again.
3. With ‘Snap’ checked in [6] of Fig. D.7 [p.47], rotate the crystal image by clicking Fig. D.6 [p.47] [R]. After right-clicking the mouse on [2] T-shaped cursor’ with it adjusted such as to touch the side surface of the crystal, register this side surface by clicking Fig. D.9 [p.48] ‘Add face’ and then Fig. D.10 [p.48] [3] Add face’.
4. Register another surface of the crystal

similarly after rotating the crystal image by clicking Fig. D.8 [p.47] [R]. After repeating this procedure until the crystal outline as shown in Fig. D.20 [p.50], ‘Exit’ on the lower right of Fig. D.20 [p.50] should be clicked to obtain the crystal 3D outline data.

D.2 Beginning of making 3D data of crystal shape

Optical images of the crystal should be taken by referring to the description in §6.2 [p.17] of Chapter 6. If ‘Record movie during dc. [3]’ is checked and angular step of ϕ axis when taking optical images of the crystal is input with an integer (1 ~ 6) in the right text box in Fig. 6.3 [p.15], Fig. 6.5 [p.16] has been displayed to automatically take optical images of the crystal.

To obtain 3D outline data of the crystal from the optical images, at first, ‘[1] >’ should be clicked to open the menu in Fig. D.1. Then, from it, ‘Show crystal movie [2]’ should be clicked to let Fig. D.2 be displayed.

D.3 Making a ‘box’ including the crystal

In Fig. D.2 (a), [1] Optical image window’ has been shown. Its magnification ratio can be changed by clicking [2] Zoom’. The initial angle of the crystal can be changed by clicking [R] Prev < > Next’ such that it is easy to make the ‘box’ including the crystal. By checking or

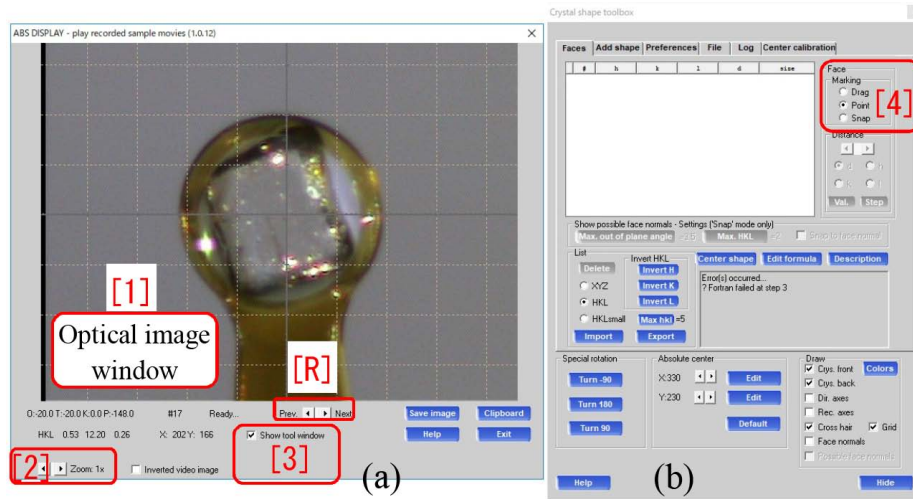


Figure D.2: Initial window of making the crystal outline data

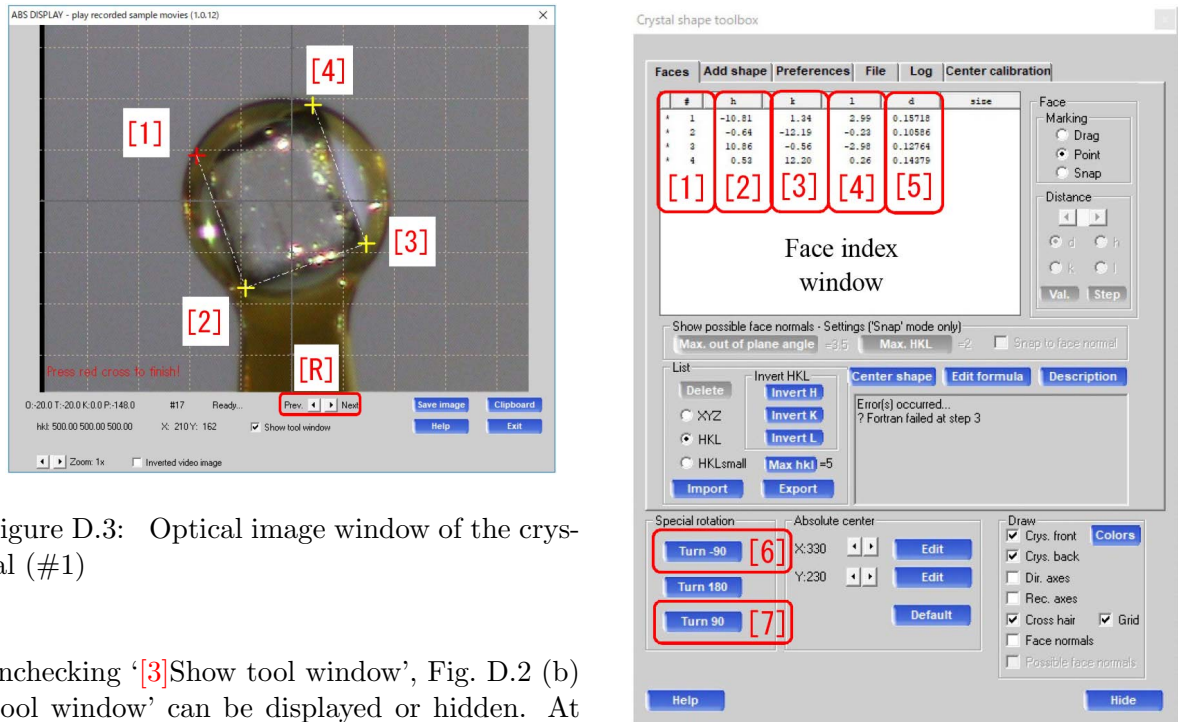


Figure D.3: Optical image window of the crystal (#1)

unchecking '[3] Show tool window', Fig. D.2 (b) 'tool window' can be displayed or hidden. At first, 'Point' should be checked in Fig. D.2 [4].

In Fig. D.3, [1], [2], [3], [4] and finally [1] again should be clicked surrounding the crystal. Then, 'Face index window' in Fig. D.4 is displayed such that ordinal numbers of #1 ~ #4 ([1]), face indices $h k l$ ([2], [3], [4]) and distances d ([5]) from the center of the crystal are displayed on it. In Fig. D.3, #1 ~ #4 correspond to planes on which the view axis and the directions of [1]-[2], [2]-[3], [3]-[4], [4]-[1] exist.

Figure D.4: Tool window #1

The normal direction of them are $ha^* + kb^* + lc^*$. Here, eq. (A.7) [p.23] in Appendix A should be referred with regard to fundamental reciprocal lattice vectors \mathbf{a}^* , \mathbf{b}^* and \mathbf{c}^* .

Then, 'Turn 90 [7]' in Fig. D.4 should be clicked to rotate the crystal image by 90° as shown in Fig. D.5 [p.47].

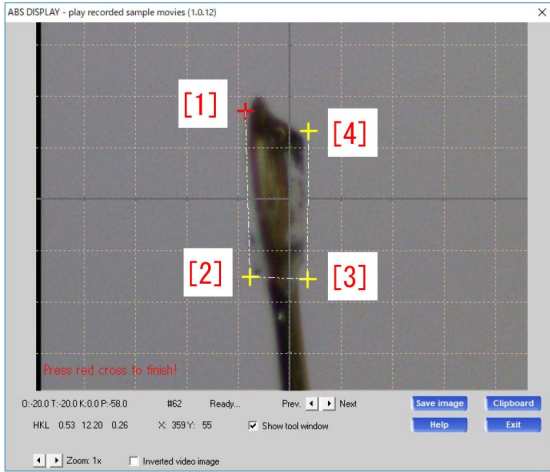


Figure D.5: Optical image window of the crystal (#2)

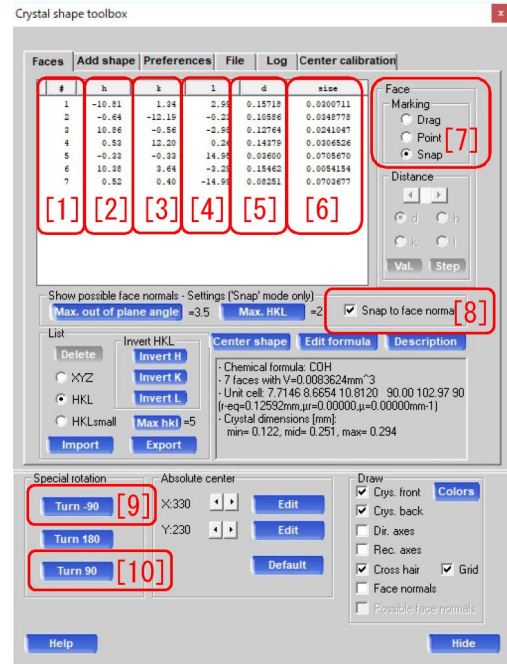


Figure D.7: Tool window #2



Figure D.6: Optical image window of the crystal (#3)

Here, [1], [2], [3], [4] and [1] again should be clicked to make the 'box' as shown in Fig. D.6 [p.47].

D.4 Trace of the crystal facet with T-shaped cursor

In Fig. D.7, the sixth parameter ([6]) size [mm²], area of the planes has been newly added. [R] in Fig. D.6 can be clicked to rotate the crystal image such that Fig. D.8 is displayed. '[1] Orientation guide' is shown with a one-dot chain line whose indices are (0, -1, 0). The mouse

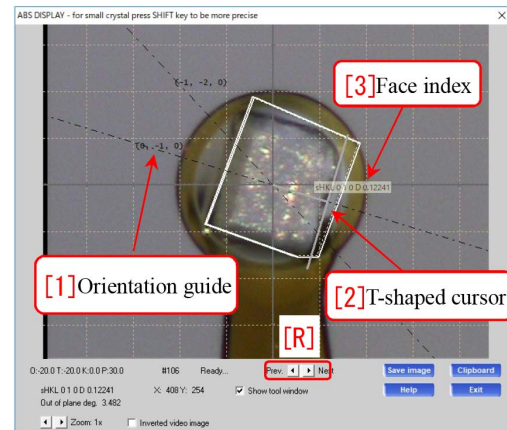


Figure D.8: Optical image window of the crystal (#4)

can be clicked on the image window to let '[2] T-shaped cursor' be displayed. This cursor should be touched to the crystal side surface with indices of 0 1 0 kept to be shown. Then, it should be right-clicked to open Fig. D.9. Here, 'Add face' should be clicked to open Fig. D.10. After verifying the orientation of the side surface '0 1 0 [1]' and its distance from the crystal center '0.12241 [2]' [mm], '[3] Add face' should be clicked. In 'Face index window' of Fig. D.11, #8 $hkl = 0.00\ 1.00\ 0.00$ has been newly added,

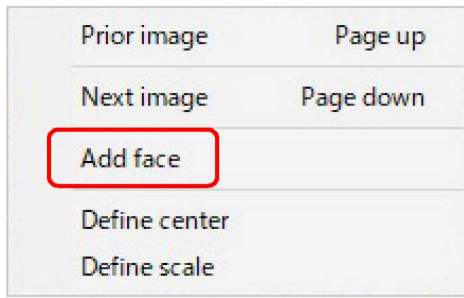


Figure D.9: 'T-shaped cursor' in Fig. D.8 has been right-clicked

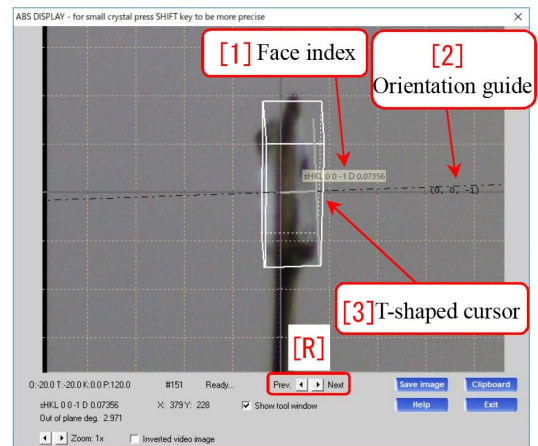


Figure D.12: Optical image window of the crystal (#5)

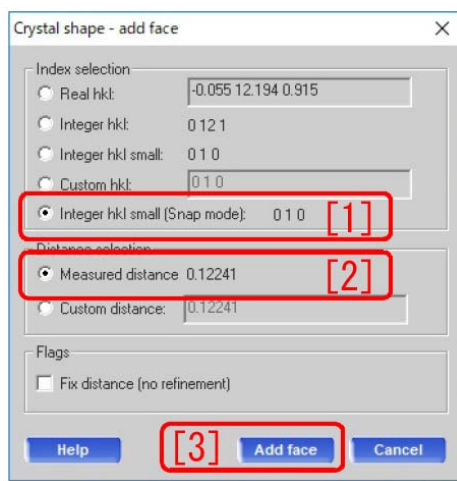


Figure D.10: Add face window (#1)

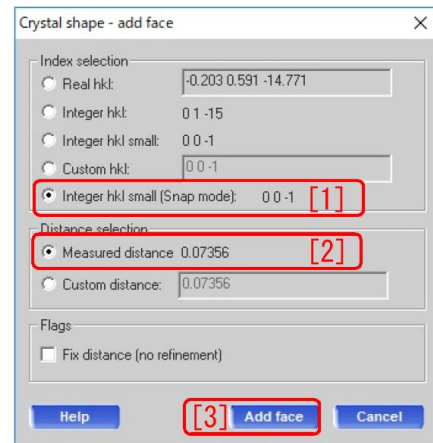


Figure D.13: Add face window (#2)

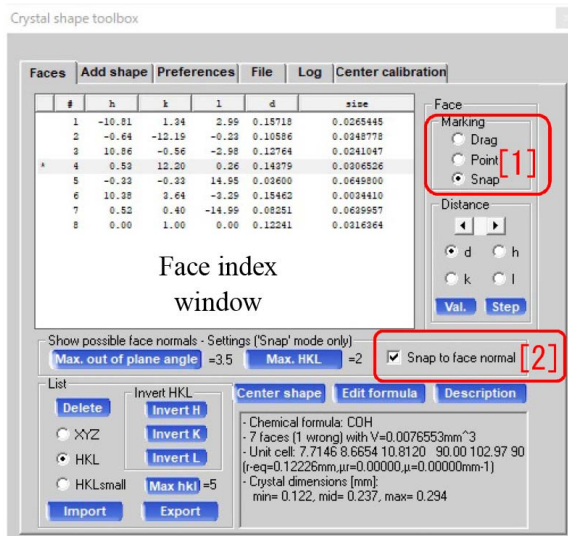


Figure D.11: Tool window #3

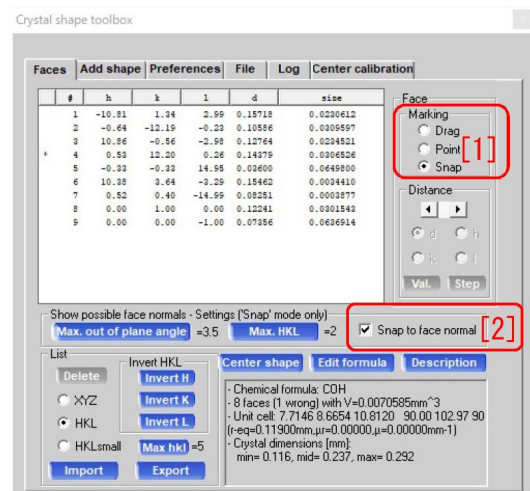


Figure D.14: Tool window #4

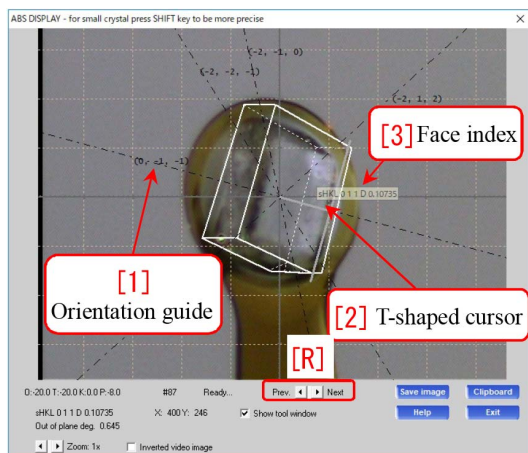


Figure D.15: Optical image window of the crystal (#6)

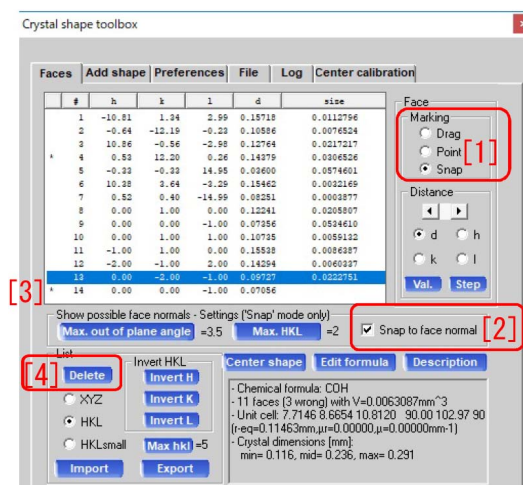


Figure D.18: Tool window #6

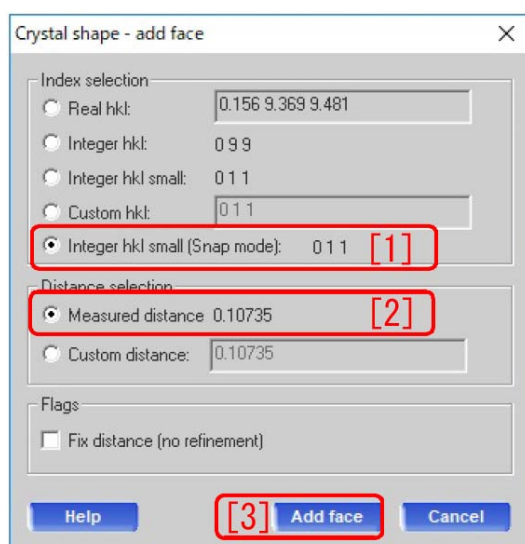


Figure D.16: Add face window (#3)

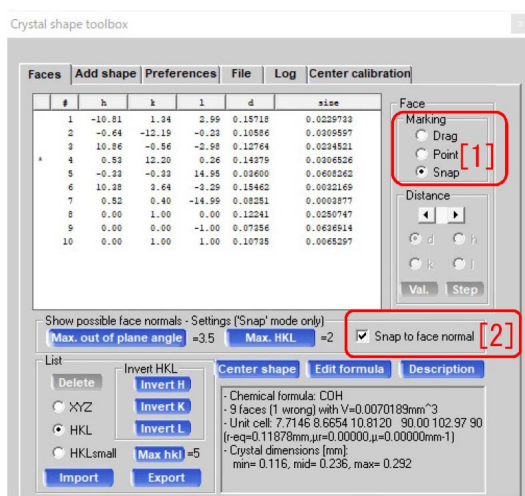


Figure D.17: Tool window #5

which shows this side surface is registered.

The other side surfaces can be registered similarly by clicking '[R] Prev < > Next' to rotate the crystal image.

0 0 $\bar{1}$ surface as shown in Figs. D.12 [p.48], D.13 [p.48] and D.14 [p.48], and 0 1 1 surface as shown in Figs. D.15, D.16 and D.17 can be added to the registrations.

In the same manner, the 3D outline shape can be improved.

D.5 Cancellation of double registration of the crystal face

In Fig. D.18, #14 0 0 $\bar{1}$ surface is attempted to add but rejected since the same surface has already been registered as #9. In this case, both #14 and #9 should be deleted by clicking '[4] Delete' in Fig. D.18 or typing 'Delete Key'. Then, 0 0 $\bar{1}$ surface should be traced again.

D.6 Edit of the crystal outline data

In Fig. D.18, '*' is marked on the left side of #4 with indices 0.00, 12.00, 0.04 since the ratio of these indices is almost the same as #8 0.00, 1.00, 0.00. Then, #4 0.00, 12.00, 0.04 should be deleted.

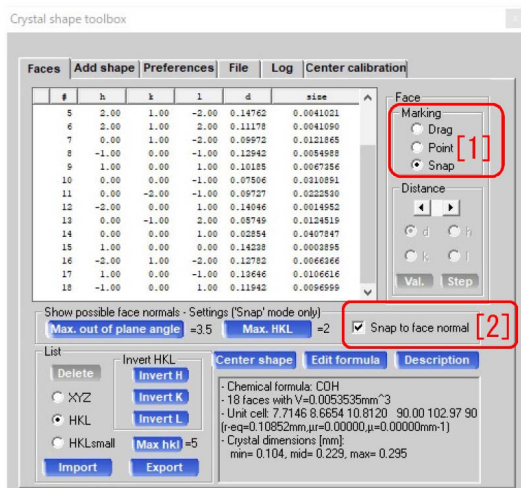


Figure D.19: Tool window #7

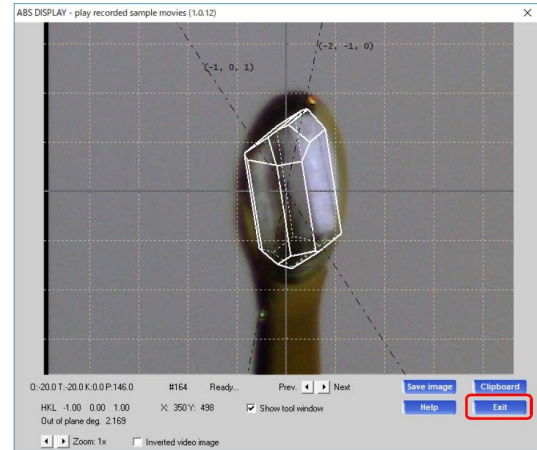


Figure D.20: Optical image window of the crystal (#7)

D.7 Registration of the crystal outline

In Fig. D.19, surfaces of indices with not integers have been deleted such that all indices are integers. Then, the 3D outline data registration can be finished by clicking 'Exit' on the lower

right corner.

The 3D outline data obtained as described in this chapter will be used for numerical absorption correction. It is applied by clicking '[5]OK' in Fig. 6.15 [p.19] of Chapter 6 when 'Faces' has been clicked in 'Numerical absorption [4]' in Fig. 6.15 [p.19].

Appendix E

Restart of the goniometer driver

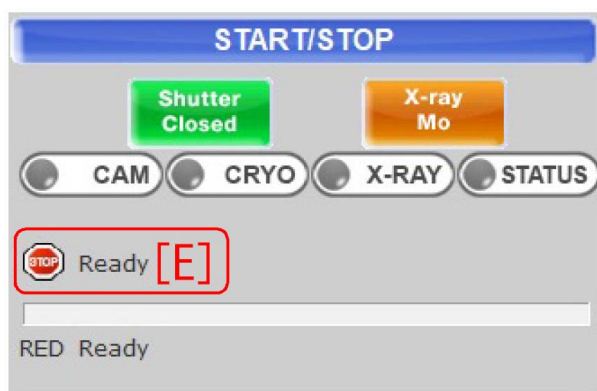


Figure E.1: Error message of the goniometer driver



Figure E.2: The whole figure of the apparatus

E.1 Concerning the error of the goniometer driver

The error message as shown in Fig. E.1 [E] (Fig. 0 [E] on the cover of this manual) appears with a moderate frequency. The procedure to recover from it is as follows.

‘×’ on the upper right of Fig. 0 on the cover of this manual can be clicked to finish the CrysAlis^{Pro}.

E.2 Shutdown and restart of the goniometer driver

‘[1] Right front panel’ in Fig. E.2 can be opened to find the goniometer driver of Fig. E.3. Its ‘[1] Power switch’ can be turned off to shut down it. After waiting for about ten seconds, it should be turned on again.



Figure E.3: The goniometer driver

E.3 Restart of the ‘CrysAlis^{Pro}’

The CrysAlis^{Pro} should be restarted to do again the procedure as described in §2.1 [p.3].

End of the document.

Index

Symbols			
2_1 screw axis	29, 32	Crystal system	28
<i>A</i> base-centered lattice	32	Crystl system	29
<i>B</i> base-centered lattice	32	Cubic	27
<i>C</i> base-centered lattice	32	D	
<i>c</i> glide plane	29, 32	D amino acid	31, 35
<i>n</i> glide plane	32	D-body	14
'Face-centered monoclinic'	27	Dell computer	i
3D data of the crystal shape	45	Determination of space group	26, 27
A		Diffraction spots	12
<i>Aba2</i> (#41)	30	Drawing of Miller	25
<i>Abm2</i> (#39)	30	Dry nitrogen	1
Absolute structure	14, 18	E	
Add face window	48, 49	Empirical absorption correction	18
<i>Ama2</i> (#40)	30	Error message of the goniometer driver	i, 51
<i>Amm2</i> (#38)	30	Ewald, P. P.	22–24
Around the goniometer head	7	Ewald construction	22–24
Auto button	i	Ewald sphere	22, 24
B		Ewald's reflection condition	24
Base-centered lattice	32, 33	Extinction rule	22, 26, 27, 29, 34
Body-centered lattice	34	F	
Body-centered monoclinic lattice	28	Face-centered lattice	34
Bragg reflection plane	24	FrameGrabber	1
Bragg's reflection condition	22, 24, 28	FrameGrabber PC	1
Bravais lattice	27, 28	Friedel's law	14, 18
C		Fundamental reciprocal lattice vector	46
<i>C12/c1</i>	31, 32	G	
<i>C2/c</i> (#15)	31, 32	Glide plane	32–34
Camsrver	1, 2	Goniometer head	7
Cell choice	29	Graphic symbol of 2_1 screw axis	29
Change of the value of Theta	4	Graphic symbol of <i>c</i> glide plane	29
Chirality	14	Graphic symbol of symmetric center	29
Choice of the account	4	H	
Choice of the X-ray source	3	H-M full notation	29, 30, 32
Choice or creation of account	3	H-M notation	29–31
Collection of diffraction intensities	14	Hermann-Mouguin full notation	29, 30
Completeness	14	Hermann-Mouguin notation	29–31
Complex lattice	28, 29, 33	Hexagonal	27
Creation of a new account	4	High-speed two-dimensional detector	1
Crystal mount window	6	Horizintal translation	i
Crystal outline data	46–50		

Humidity in the detector	1, 2	$P2_1/c$ (#14)	27
		$P2_1/c11$	30
I		$P2_1/n11$	30
Image due to 2_1 screw axis	29	$P2_111$	32
Image due to c glide plane	29	$P2_12_12_1$ (#19)	31, 32
In-plane rotation	i	$P3_121$ (#152)	39
Initializing	3	$P6_122$ (#178)	41–43
		$P\bar{1}$ (#2)	31, 32
L		Password	i
L amino acid	31, 35	Phase problem	29, 31
L-body	14	Position of atom	29
Laue, M. T. F. von	22, 23	Pre-Experiment	12
Laue group	14, 27–29	Pre-experiment window	3
Laue's reflection condition	22–24	Primitive lattice	28
Level of screening result	8	Primitive translation vector	23
Liquid paraffin	7	process.out	27
Login name	i		
		R	
M		R-body	14
Magnet base	6	Racemic compound	31
Measurement menu	11	Reasonableness of using four indices	39
Menu of 'Crystal tab'	45	Reciprocal lattice	22–24
Micromount	6	Reciprocal lattice vector	24
Miller indices	25	Reciprocal space	23, 24
Molecular model	10, 11	Recovery from the error	i, 51
Monoclinic	28, 31	Redundancy	14
Monoclinic	8, 14, 27, 28, 30, 32	Remote desktop	1, 2
Mount of the crystal	6	Resolution	14
Mount window	4	Restart of the goniometer driver	51
		Result of screening	8
N		S	
Nishikawa, S.	28	S-body	14
O		Schönflies notation	29
Optical image window of the crystal	16	Screening of the crystal	6
Optical images taking window	18	Screening option window	8
Optical isomer	35	Screw axis	29, 32, 33, 36, 37, 39
Ordinal number of space group	29	Shutdown options	20
Orthorhombic	27, 32	Six-fold screw axis	39
		SM Screening tab	3
P		SM Screening window	3, 6–8, 10, 12
$P112_1$	32	Space group	11, 18, 26–29
$P112_1/a$	30	Special Collection window	16
$P112_1/b$	30	Startup of the CrysAlis ^{Pro}	3
$P112_1/n$	30	Status of Pre-experiment	12
$P12_1/a1$	30, 31	Strategy	10, 14
$P12_1/c1$	30, 31	Strategy window	15
$P12_1/n1$	30, 31	Sucrose	i
$P12_11$	31, 32	Symmetric center	29, 32
$P2_1$ (#4)	11, 31, 32	Symmetric element	28
$P2_1/b11$	30	Symmetry	22
$P2_1/c$ (#14)	26–28, 30, 31		

T		Unique axis	29
T-shaped cursor	47, 48		
Taurine	26–28	V	
Tetragonal	27	Vertical translation	i
The power switch of the goniometer driver	51	W	
Three-fold screw axis	39	WIT	10
Tool window	46–49	WIT window	10
Triclinic	27, 32	Wyckoff, R. W. G.	28
Trigonal	27	Z	
U		Zoom	i